

## Belomorian drusite (coronite) complex, Baltic Shield, Russia: An example of dispersed intrusive magmatism in early Paleoproterozoic mobile zones

E. V. Sharkov, I. S. Krassivskaya, and A. V. Chistyakov

Institute of Geology of Ore Deposits, Petrography, Mineralogy, and Geochemistry (IGEM), Russian Academy of Sciences, Moscow, Russia

**Abstract.** The Early Paleoproterozoic (2.46–2.36 Ga) Belomorian drusite (coronite) complex was addressed to for the first time in discussing the geology, petrology, and genetic conditions of dispersed intrusive mafite–ultramafite magmatism that developed in intercratonic mobile zones and granulite belts of Early Precambrian age. The complex comprises numerous small rootless synkinematic intrusions that are scattered throughout the Belomorian Mobile Belt (BMB). The rocks of the complex are compositionally close to the rocks of large layered intrusions in the neighboring cratons and compose, together with them, the Baltic Large Igneous Province (BLIP) of the silicic high-Mg (boninite-like) series. It is demonstrated that the magma generation regions were similar beneath the cratons and BMB, but, in contrast to the situation at the cratons, melt portions ascending from below the BMB could be accommodated only in small chambers, whose position was controlled by local heterogeneities induced by the tectonic flowage of the host rocks. Moreover, these chambers continuously changed their position, thus precluding the origin of large bodies and eventually giving rise to dispersed magmatism. Upon their crystallization, the intrusions were affected by metamorphic reworking under amphibolite-facies conditions, so that weakly altered rocks are now preserved only in the cores of these bodies. The rocks are characterized by the development of drusite (coronite) textures along the grain boundaries of primary magmatic minerals.

### Introduction

Lately it became more and more obvious that magmatic processes were significantly different in the Early Precambrian and Phanerozoic. In this sense, a remarkable and unique period in the Earth's evolution was the Early Paleoproterozoic (2.5–2.2 Ga), when the overall Earth's cooling produced a rigid crust susceptible to brittle deformations [Bogatikov *et al.*, 2000]. The predominant types of igneous rocks were then the rocks of the silicic high-Mg (boninite-like) series (SHMS) of mantle–crustal genesis, which were

compositionally close to Phanerozoic island-arc series but originated in absolutely different tectonic environments [Sharkov *et al.*, 1997].

The principal Early Paleoproterozoic tectonic structures of the Baltic Shield were rigid Archean Karelian and Kola cratons, which were separated by the Lapland–Umba Granulite Belt (LUGB) (Figure 1). Its boundaries with neighboring cratons were marked by the development of intercratonic mobile belts: Belomorian (BMB) in the southwest and Tersk–Lotta (TLMB) in the northeast [Sharkov *et al.*, 2000]. The cratons were uplifted extending areas with SHMS mantle-related magmatism, whereas LUGB was a compensation compressed subsiding structure with crustal synkinematic enderbite–charnockite magmatism. The transitional mobile belts constrained between them were zones of low-angle tectonic flowage in an extensional environment. These zones were composed mostly of tectonic slabs of Archean rocks detached from the neighboring cratons and were characterized by specific dispersed intrusive SHMS

Copyright 2004 by the Russian Journal of Earth Sciences.

Paper number TJE04148.  
ISSN: 1681–1208 (online)

The online version of this paper was published 27 June 2004.  
URL: <http://rjes.wdcb.ru/v06/tje04148/tje04148.htm>

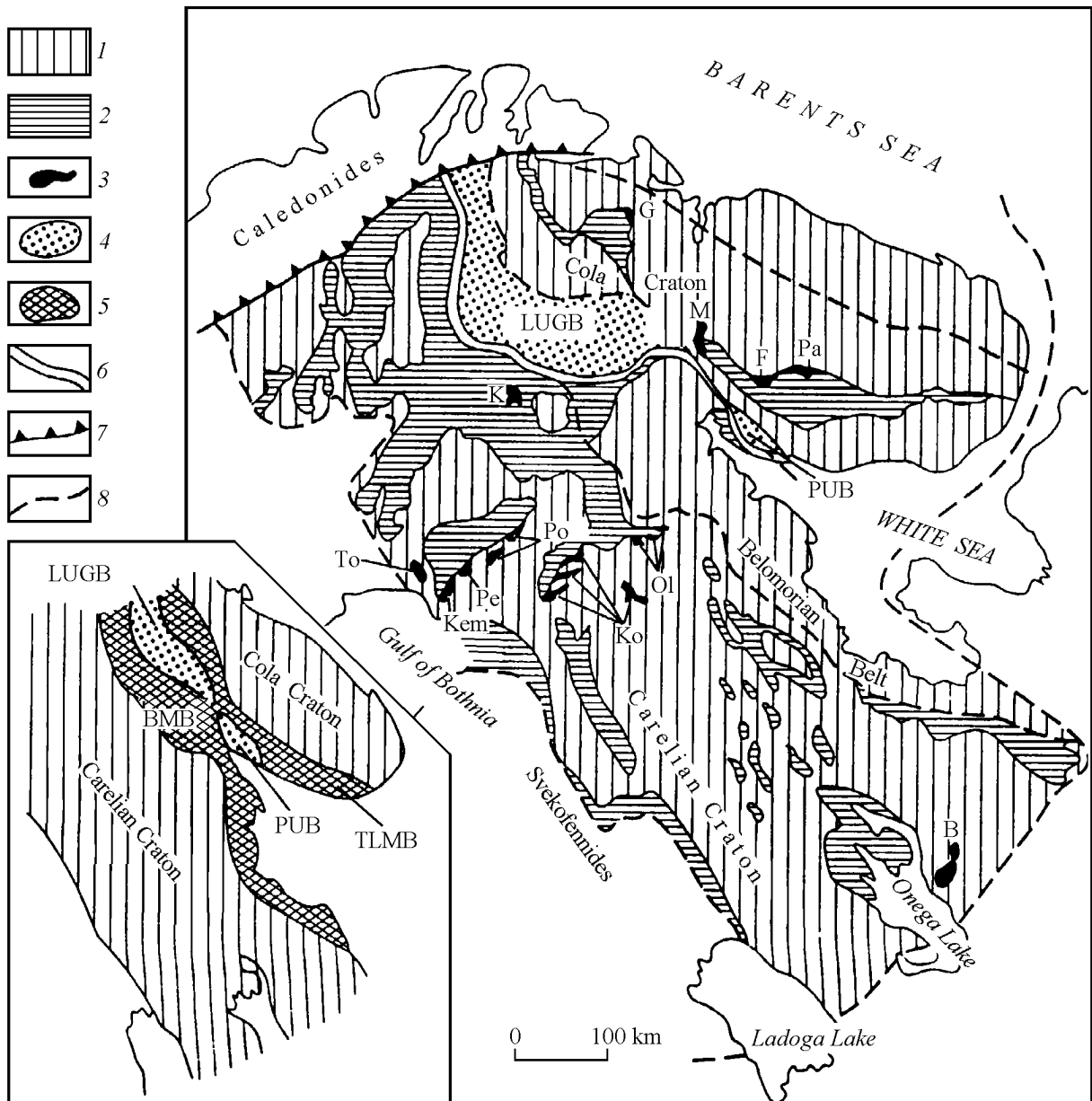


**Figure 1.** Early Paleoproterozoic Baltic large igneous SHMS province (after [Sharkov et al., 1997]).

1 – Archean basement; 2 – Paleoproterozoic sedimentary-volcanic complexes; 3 – layered intrusions: B – Burakovsky, G – Mt. General'skaya, K – Koitilainen, Kem – Kem', Ko – Koilismaa, M – Monchegorsky, Ol – Olanga (Oulanka) group, Pa – Pana, F – Fedorova Tundra; 4 – Lapland-Umba granulite belt, LUGB (PUB – Por'ya Bay-Umba Block); 5 – intercratonic mobile belts (BMB – Belomorian, TLMB – Tersk-Lotta); 6 – Main Lapland Thrust; 7 – major faults; 8 – eastern boundary of the Baltic Shield. The inset shows the position of major structural domains in the eastern part of the Baltic Shield in Early Paleoproterozoic time.

magmatism, to which this paper is devoted. All of these principal tectonic structures developed simultaneously and were related to the regional metamorphic zoning, in which deformations and the metamorphic grade increased from the cratons toward the granulite belts [Sharkov et al., 2000].

For our purposes, it is most interesting to trace corre-

lations between magmatic processes that occurred simultaneously in different tectonic environments: (i) in rigid cratons and (ii) intercratonic transitional mobile belts between cratons and the LUGB in the Baltic Shield. In both situations, these processes produced SHMS of the Baltic large igneous province (BLIP), which was dated at 2.55–2.35 Ga

[*Sharkov et al.*, 1997], but the character of the processes in these environments was basically different. In cratons, they generated large layered intrusions, dike swarms, and volcano-plutonic complexes in riftogenic structures (such as Pechenga–Varzuga and the Vetrenyi Belt). Conversely, in intercratonic mobile belts, these processes produced mostly numerous small synkinematic intrusions of mafic and ultramafic rocks disseminated throughout the area of the belts.

Within the BMB, these bodies are always variably metamorphosed and transformed into so-called drusites (this local term was coined by E. S. Fedorov in 1905 to denote coronitic metagabbro). In the course of regional metamorphism, reactions between the mafic magmatic minerals of these rocks and their plagioclase brought about concentric rims of metamorphic minerals (mostly clinopyroxene, hornblende, and garnet). Rocks of the drusite complex were thoroughly studied by many geologists and petrologists, among whom we would like to mention N. G. Sudovikov, K. A. Shurkin, G. M. Saranchina, L. A. Kosoi, V. L. Duk, F. P. Mitrofanov, M. M. Efimov, N. D. Malov, V. S. Stepanov, A. I. Slabunov, and others.

The isotopic dating of most of the massifs (see below) has demonstrated that the magmatic crystallization ages fall within the range of 2.45–2.36 Ga, while the development of corona textures was related to the Karelian (Svecofennian) metamorphic cycle at  $\sim 1.85$  Ga [*Alexeev et al.*, 1999; *Bibikova et al.*, 2001]. The precise SHRIMP dating of zircon from all ortho- and para-rocks of the Belomorian Group [*Bibikova et al.*, 2004] indicates that no metamorphic events occurred after the emplacement of the gabbroid complex but before the Karelian cycle. Petrological analysis demonstrates that phase equilibria in the coronites, the chemistry of their metamorphic clinopyroxene and garnet, and the P–T metamorphic parameters are fully identical to the analogous values characteristic of the Karelian prograde metamorphism in the host garnet–clinopyroxene amphibolites [*Korikovsky*, 2004; *Larikova*, 2000] and were  $T = 650\text{--}700^\circ\text{C}$  at  $P > 6$  kbar [*Larikova*, 2000]. The pressure value was lately reevaluated by *Korikovsky* [2004] at 9–10 kbar.

For the purposes of this publication, it is important to stress that the process of gabbro coronitization was apparently isochemical, when magmatic textures and relics of magmatic olivine, orthopyroxene, and plagioclase, as well as magmatic structures, such as layering, etc., remain well preserved in spite of the wide spreading of embryonic or well-developed orthopyroxene, clinopyroxene, and garnet rims. All of the petro- and geochemical samples used in this research were taken from massive, mostly coronitized gabbroids and ultramafics, which are comagmatic with these rocks but were less affected by younger shearing and show no petrological evidence of overprinted metasomatism and component migration. Because of this, it is assumed that all geochemical features of the mafite–ultramafite complex correspond to its primary magmatic nature.

In contrast to magmatism in cratons, which has been studied fairly thorough, dispersed magmatism of intercratonic mobile belts remains known inadequately little. At the same time, these processes are a specific manifestation of endogenic activity, whose understanding provide better in-

sight into the distinctive features of Precambrian magmatic processes. Since this paper is devoted to the magmatic (pre-coronite) history of the mafic rocks, the prefix meta will be used below only when strongly altered rock varieties are addressed to.

## Geology of the Belomorian Drusite Complex

The drusite complex comprises multiple small (from a few hundred meters to 1–2 km long or, rarely, larger) bodies, which range from tens to hundreds of meters in thickness. These are rootless mafic and ultramafic (more rarely, intermediate) intrusions, which are widespread laterally within high-grade metamorphic rocks of the BMB [*Shurkin et al.*, 1962]. The intrusions are dominated by norite and gabbronorite bodies with subordinate amounts of ultramafics (plagioclase harzburgites, bronzitites, websterites, and predominant plagioclase lherzolites), anorthosites, and magnetite gabrodiorites. The intrusions number in the tens of thousands [*Malov and Sharkov*, 1978]. The relative abundances of different rock types in the complex, calculated over an area of about 6000 km<sup>2</sup> in northern Karelia by N. D. Malov and refined during later studies, are as follows:  $\sim 16\%$  for ultramafics, 30% for olivine norites and gabbronorites, 20% for gabbronorite-anorthosites and anorthosites, and  $\sim 4\%$  for magnetite gabrodiorites and diorites. This roughly corresponds to the abundances of the same rock types in large mafic–ultramafic intrusion in neighboring cratons (Monchegorsk, Burakovsky, Koilismaa, and others), with which they are also similar petrographically and geochemically, but these rocks in the drusite complex are obviously prone to form individual bodies.

An analogous style of Early Paleoproterozoic magmatic activity is typical of the coeval Tersk–Lotta Mobile Belt. This belt also includes numerous small synkinematic bodies of mafic and ultramafic rocks, which were affected by younger metamorphic reworking. These bodies are known south of the Pechenga and Imandra–Varzuga structures and are most typical of the Monchegorst district [*Belyaev and Kozlov et al.*, 1967; *Smolkin et al.*, 2004] and the southern foothills of the Chuna-Tundra Range [*Mitrofanov and Pozhilenko*, 1991]. Judging by the isotopic dates of these rocks, they are of the same age as the Belomorian drusites [*Bayanova et al.*, 2002].

Only the largest intrusions in both belts show primary magmatic layering, with the footwalls of these bodies sometimes made up of peridotites and pyroxenites and their hanging walls consisting of gabbroids. However, the most widespread bodies consist only of one of the main rock types. These bodies usually have the shapes of distorted ovals, often with tectonic contacts and marginal parts metamorphosed to the amphibolite facies, with relatively little altered rocks usually preserved in their cores. Primary intrusive contacts are much more rare and are marked with chilled zones, apophyses, and eruptive breccias with host-rock xenoliths.

Judging from the best preserved bodies of the complex,

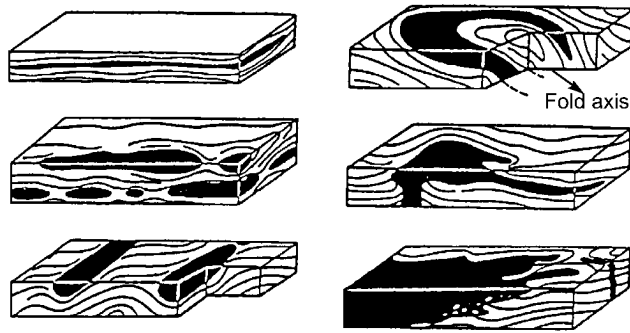


**Figure 2.** Morphology of drusite intrusions (after [Shurkin et al., 1962]).

they could originally have the morphologies of irregular lenses, sills and dikes or, in places, horseshoes (in map view), filling the detachment space in the hinges of relatively large folds (Figure 2). This provides grounds to hypothesize that the melt was emplaced simultaneously with deformations in the host rock, which is consistent with the results of statistical studying of the distribution of Belomorian drusite intrusions [Malov and Sharkov, 1978]. These bodies were determined to definitely group along permeable zones of

northwestern, northeastern, or, more rarely, northern and western trend (Figure 2), i.e., directions coinciding with the predominant orientation of deformations in the Early Paleoproterozoic [Volodichev, 1990].

#### Some Examples of the Structures of the Mafites–Ultramafite Bodies

According to their composition, the intrusions are subdivided into two types: (1) predominantly mafic (gabbro-norite–anorthosite) and (2) predominantly ultramafic (lherzolite–gabbro-norite). Examples of their inner structures will be considered below. Generally, the distribution of drusite bodies according to their composition shows no clear zoning: as can be seen from Figure 3, even small portions of the bodies sometimes include all rock types that are typical of the whole Belomorie region, where from one to three intrusions on average are usually exposed within 1 km<sup>2</sup> area.

#### Bodies Mafic Rocks (Gabbro-norite–Anorthosite)

The anorthosite body of Pezhostrov Island of the Keret' Archipelago in the White Sea has a roughly rectangular

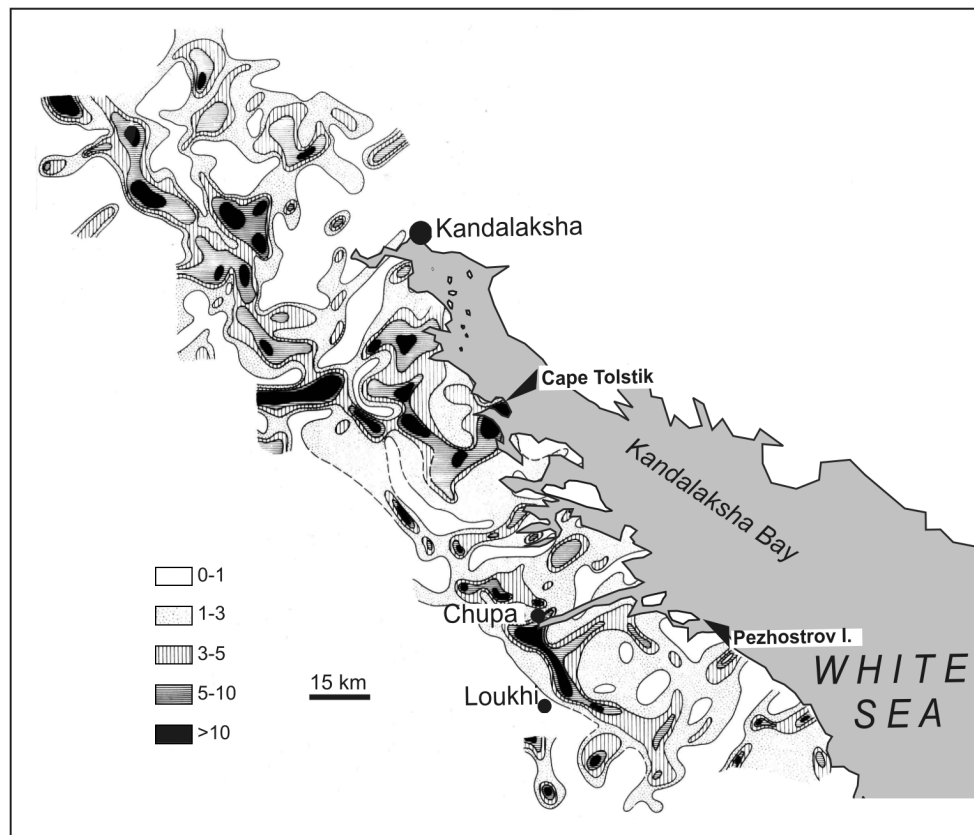


**Figure 3.** Schematic map showing the distribution density (percentage of the total area) of drusite massifs in the Belomorian Mobile Belt (modified after [Malov and Sharkov, 1978]).

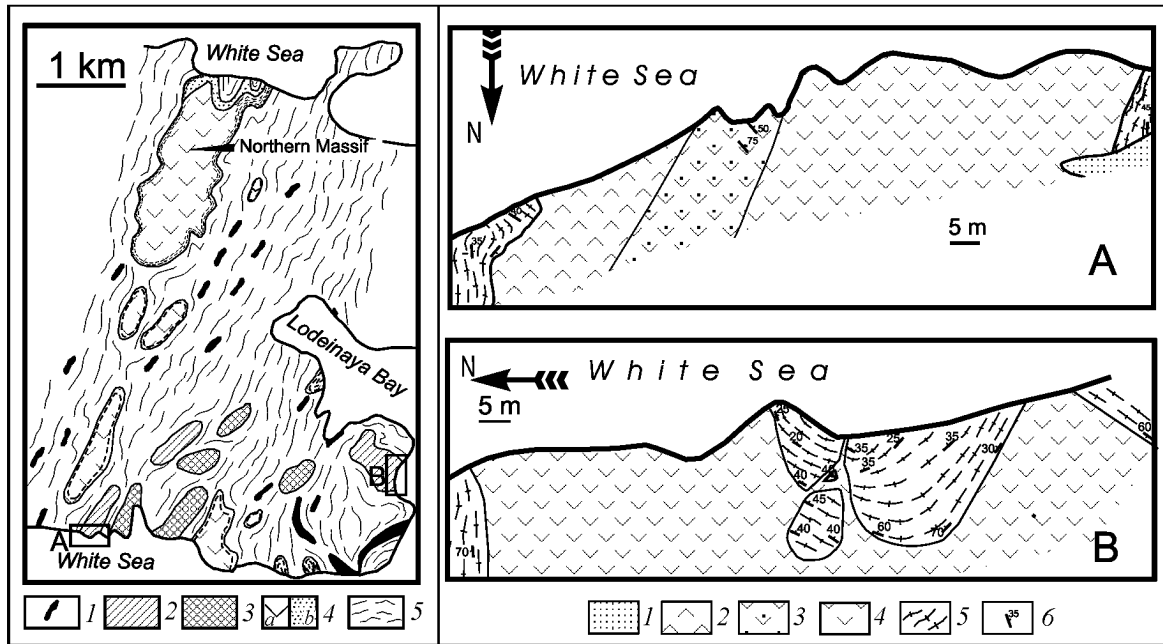


**Figure 4.** Schematic geological map of the central part of Pezhostrov Island, Keret' Archipelago, White Sea (prepared by E. V. Sharkov and A. V. Chistyakov using materials provided by V. L. Duk).

1 – Lens- and dike-shaped bodies of garnet amphibolites; 2 – bodies of gabbronorite-lherzolites; 3 – bodies of strongly altered gabbronorites; 4 – bodies of metagabbronorite-anorthosites: (a) gabbronorite-anorthosites, (b) marginal fine- to medium-grained leucogabbronorites in the inner-contact zone of the Northern Massif; 5 – host Archean plagiomigmatites. The insets are detailed structural schemes of the coastal parts of two gabbronorite-lherzolite bodies: A – southern termination of the Southern body, and B – eastern part of the Lodeinaya Bay body. 1 – Quaternary deposits; 2 – plagioclase lherzolites; 3 – olivine gabbronorites; 4 – melanocratic gabbronorites; 5 – host gneisses and migmatites; 6 – strikes and dips of lineation.

shape ~1 km long and ~200–300 m wide and is elongated nearly northward, conformingly with the trends of the host Archean granite-gneisses (Figure 4). The geology and petrology of this intrusion were described in detail elsewhere [Sharkov *et al.*, 1994, 1999], because of which here we present only the most general information. The anorthosites are spatially restricted to the core of a gently dipping anticline. The contacts between them and the host rocks are always tectonic, except only for the northern part, where fine- to medium-grained leucogabbronorites occur, which seem to compose the inner-contact zone of the intrusion. The crystallization of the massif was dated at  $2452 \pm 20$  Ma (zircon U–Pb dating); the  $^{207}\text{Pb}/^{206}\text{Pb}$  age of the metamorphic apatite is approximately 1789 Ma [Alexejev *et al.*, 2000].

The intrusion is dominated by gabbronorite-anorthosite and contains subordinate amounts of gabbronorite. The southeastern part of the body includes magnetite gabbronorite and gabbro-diorite, which likely correspond to the uppermost part of the body. All rocks were extensively deformed and blastomylonitized under amphibolite-facies conditions and are now mostly transformed into plagioclase schists and amphibolites. The primary magmatic textures and structures are preserved only occasionally. The marginal portions of the body are reworked particularly

strongly. They were deformed, together with the host rocks, into gently dipping folds and are in places impregnated by migmatites and cut by veinlets of pink granitic material.

The blastomylonitization zones cutting across the Pezhostrov body have a complicated morphology and are often intruded by conformable mafic dikes, which are transformed into garnet amphibolites (Figure 5). Chemically, these dikes affiliate with SHMS [Sharkov *et al.*, 1994]. The morphology of the dikes, with their material forced into the hinges of folds and the absence of these dikes from more massive rocks led us to suggest that they were emplaced simultaneously with blastomylonitization of the already-solid host intrusive rocks. Analogous dikes and boudins of garnet amphibolites occur in the host gneisses (Figure 4).

The strong reworking of the intrusion obliterated its original morphology. A rough idea about it can be given by anorthosite bodies in other islands of the Keret' Archipelago (Keret', Peschanyi, Medyanka, and others), located 10–20 km northeast of Pezhostrov Island. In these islands, anorthosites occur as lens-shaped bodies from tens to a few hundred meters thick and hundreds of meters long, which are conformable with the structures of the host gneisses and migmatites. One of these bodies in Medyanka Island includes eruptive breccia, in which metagabbronorite-

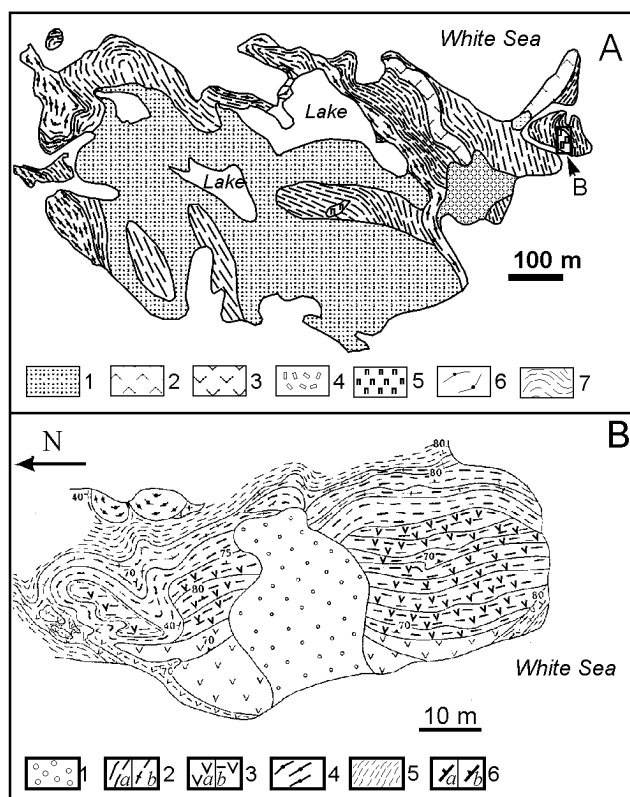


**Figure 5.** Bodies of the drusite complex in the Lodeinyi Island, Kandalaksha Archipelago, White Sea (prepared by E. V. Sharkov). A – Schematic geological map of the island. 1 – Quaternary deposits; 2 – gabbronorites and olivine gabbronorites; 3 – metagabbronorites; 4 – metagabbro-anorthosites; 5 – plagioclase lherzolite bodies; 6 – garnet amphibolites; 7 – migmatites. B – Geological structure of the drusite body (block) of layered metagabbro-anorthosites and gabbronorites. 1 – Quaternary deposits; 2 – (a) garnet amphibolites and (b) amphibolites after gabbronorite-anorthosites; 3 – variably altered (a) gabbronorites and (b) gabbronorite-anorthosites with relict magmatic textures and structures; 4 – garnet amphibolite boudins; 5 – plagiomigmatites; 6 – strikes and dips of: (a) migmatites and amphibolites after rocks of the drusite complex, (b) primary magmatic layering.

anorthosite cements angular fragments of metadiabases and stratified calc-silicate rocks (perhaps, of sedimentary origin) [Shurkin and Levkovskii, 1966]. The fragments are thought to be xenoliths of the supracrustal host rocks.

By analogy with these massifs, the Pezhostrov intrusion can be thought to have been a fragment of a larger lens-shaped body that was repeatedly affected by deformations and metamorphism and disintegrated into blocks, which were pulled apart during the plastic flow of the magmatic matrix (Figure 4).

Insight into the character of the primary layering of these bodies is provided by a small metagabbro-anorthosite body in the eastern part of Island Lodeinyi in the Kandalaksha Archipelago. The body is a large lens-shaped boudin among

migmatites (Figure 6). Its western portion consists of mostly massive gabbronorites, and the eastern part is made up of gabbronorite-anorthosites with irregularly shaped thin gabbronorite layers. The layered rocks show structures of crystalline material sliding (Figure 7), which suggest that the intrusion was emplaced under dynamic conditions. Relics of magmatic structures and minerals were found only in the central part of the body. The degree of rock blastomylonitization strongly increases toward the margins of the body, and the rocks are transformed into amphibolites and migmatized garnet-amphibolite schists.

The strongly altered metagabbro-anorthosite intrusion in the southwestern part of Anisimov Island in the Kandalaksha Archipelago has a length of >1.6 km (the length of the island itself) and a width of at least 200 m (Figure 8). All contacts of the body with the host Archean granite-gneisses and migmatites are tectonic, through zones of shearing of all rocks, to which younger migmatization is often restricted. Analogous zones divide the intrusion into large blocks, in each of which the primary rock structures remain well preserved. The blocks can be subdivided into the following two major groups:

(i) Blocks consisting of medium-grained metagabbro-anorthosites with subordinate amounts of gabbronorites (Figure 8B). Their layering is manifested in the form of relatively thin (1–3 cm) pyroxenite layers. There are traces of crystalline material sliding, resembling the complicated morphology of layers in the intrusion in Lodeinyi Island (see above).

(ii) Blocks of thinly layered rocks with alternating layers of olivine metapyroxenites and metagabbro-anorthosites. The layers are 1–2 cm, rarely up to 10 cm, thick (Figures 8B and 9). This layering in the northern part of the island acquired a lenticular character due to blastomylonitization, with pyroxenites occurring as distorted lenses (small boudins) among schists (former leucogabbroids) (Figure 9).

The relationships of these thinly layered rocks with the gabbro-anorthosites and gabbronorites are uncertain. They could be produced by additional mafic magma injections into the already rigid but still hot intrusion, as was determined for other analogous layered bodies [Sharkov, 2002]. The de-



**Figure 6.** Slip folds in layered metagabbro-anorthosite in Lodeinyi Island. Photo: M. K. Sukhanov.

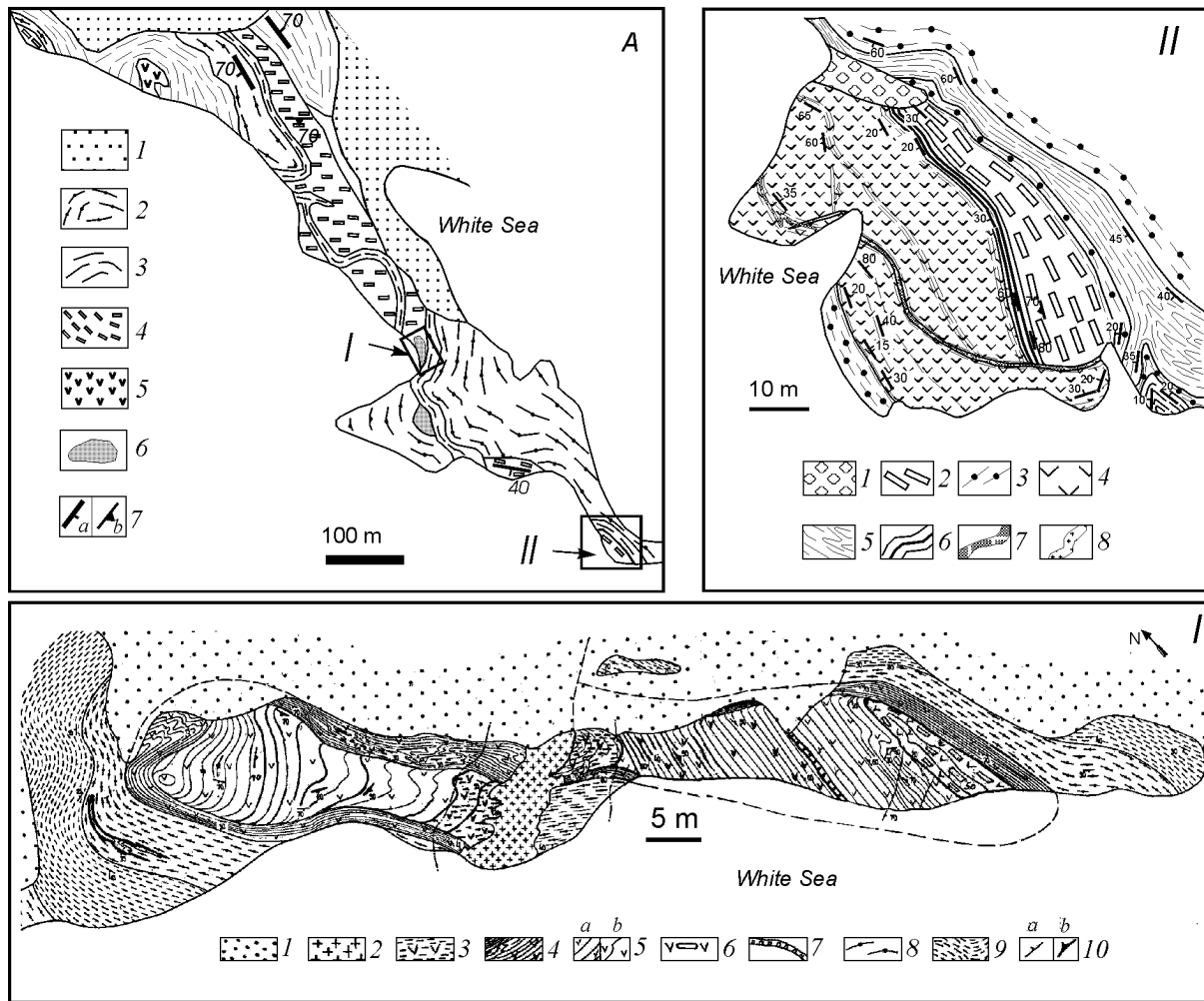


**Figure 7.** Schematic geological map of the southern part of (A) Anisimov Island (prepared by E. V. Sharkov). 1 – Quaternary deposits; 2 – garnet amphibolites; 3 – migmatites; 4 – gabbronorite-anorthosites and gabbronorites; 5 – garnet gabbro-amphibolite; 6 – blocks of thinly layered intrusive rocks; 6 – strikes and dips of: (a) gneissosity, (b) primary layering. I – Detailed map of a block of thinly layered gabbronorites. 1 – Quaternary deposits; 2 – granite pegmatites; 3 – diaphthorized thinly layered gabbroids in contact with a pegmatite vein; 4 – garnet amphibolite developing after gabbroids; 5 – thinly layered gabbroids: (a) thinly layered gabbronorite and pyroxenites (see Figure 9a), (b) boudinaged thin layering in the northern part of the body (see Figure 8b); 6 – metagabbronorite-anorthosites; 7 – olivine pyroxenite dike (see Figure 10); 8 – garnet amphibolites; 9 – migmatites; 10 – strikes and dips of: (a) gneissosity, (b) primary layering. II – Detailed map of a leucocratic gabbroid block. 1 – Quaternary deposits; 2 – gabbronorite-anorthosites; 3 – gabbronorites; 4 – thin zones of rhythmically intercalating gabbronorites and gabbronorite-anorthosites; 5 – garnet amphibolites; 6 – migmatites; 7 – diabase dike.

velopment of the thin layering was, perhaps, caused by the flow of the melt before its complete crystallization. The genesis of this layering is considered in detail in the aforementioned paper.

The rocks composing the blocks are metamorphosed and contain newly formed garnet and green hornblende, with magmatic minerals occurring merely as relics. The thinly layered rocks of the blocks include a plagioclase olivine websterite dike metamorphosed to the same metamorphic grade. The primary contacts of the dike have a complicated mor-

phology, and the dike was emplaced conformably with the layering (Figure 10). Unlike the Pezhostrov Massif, this dike was obviously intruded before shearing: as can be seen in Figure 8, the blastomylonite zone truncates both this dike and the host sheared gabbroids.

Although the blocks of thinly sheared rocks are elongated northwestward (conformably with the general trends of the migmatites), their layering is oriented roughly westward. An analogous orientation of layering is also characteristic of the gabbronorite-anorthosites occurring north and south of this

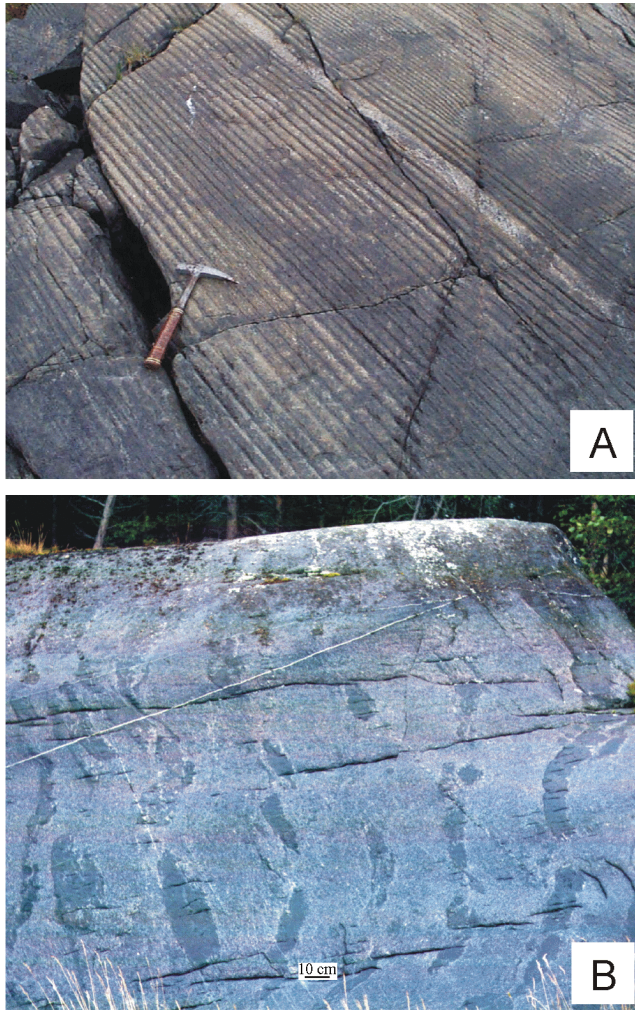


**Figure 8.** Thin primary layering in Block II of the Anisimov Island body (see Figure 7). A – Thinly intercalating metagabbronorites and metapyroxenites; B – “lenticular” layering. Photo: A. V. Chistyakov.

body (Figure 8). This suggests that the Anisimov Island anorthosite massif originally trended northward and dipped southward. The modern morphology of its fragments seems to have been caused by its dividing into blocks of predominantly northwestern trends in the process of the ductile flowage of the magmatic matrix during later evolutionary stages of the BMB.

The inner structure of the drusite body in Voronii Island (Figure 11) is characterized by the predominance of gabbronorite–anorthosites with thin gabbronorite layers. The layering trends to the northwest and dips at low (20°–30°) angles to the northeast. The western and northern inner contacts of the body are marked by unequally grained gabbronorites, whose composition and texture are close to those of rocks in the marginal zone of the Pezhostrov body (see above). All contacts with the host migmatites are tectonic, with nearby migmatites containing lens-shaped drusite xenoliths.

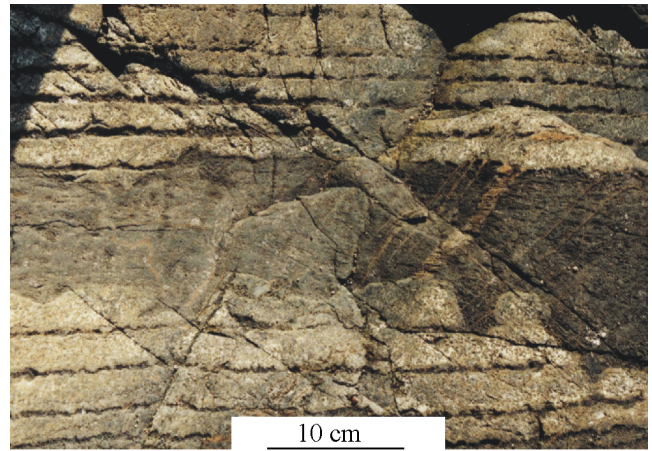


**Figure 9.** Olivine orthopyroxenite dike in thinly layered gabbronorites, Anisimov Island. Photo: A. V. Chistyakov.

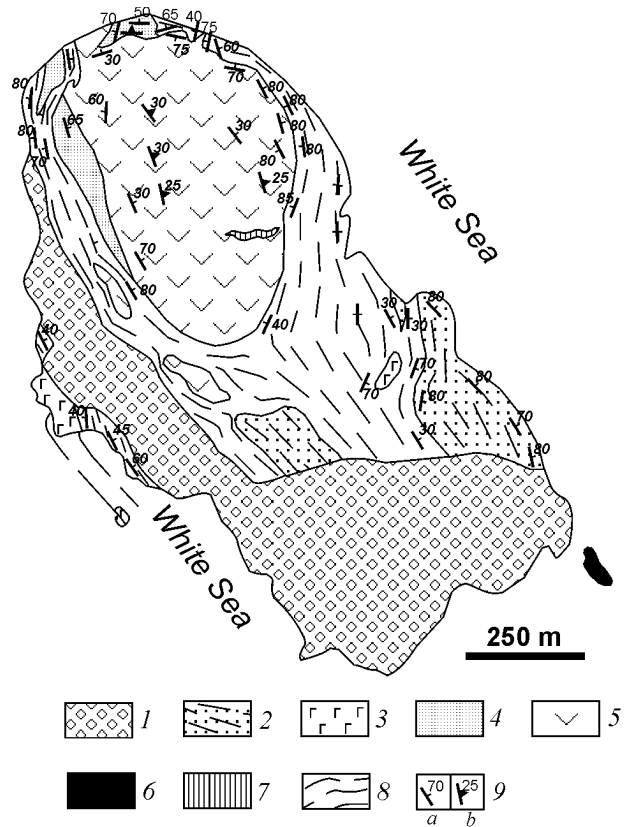


**Figure 10.** Geological map of Voronii Island, Kandalaksha Archipelago, White Sea (prepared by E. V. Sharkov partly using materials of F. P. Mitrofanov [Shurkin et al., 1960]). 1 – Quaternary deposits; 2 – garnet amphibolites (sometimes with relict volcanic structures); 3 – bodies of melanocratic gabbronorites and plagioclase lherzolites; 4 – unequally-grained leucocratic gabbronorites; 5 – gabbronorite–anorthosites; 6 – block of thinly layered rocks; 7 – granite pegmatites; 8 – Archean gneisses and migmatites; 9 – strikes and dips of: (a) primary layering, (b) gneissosity.

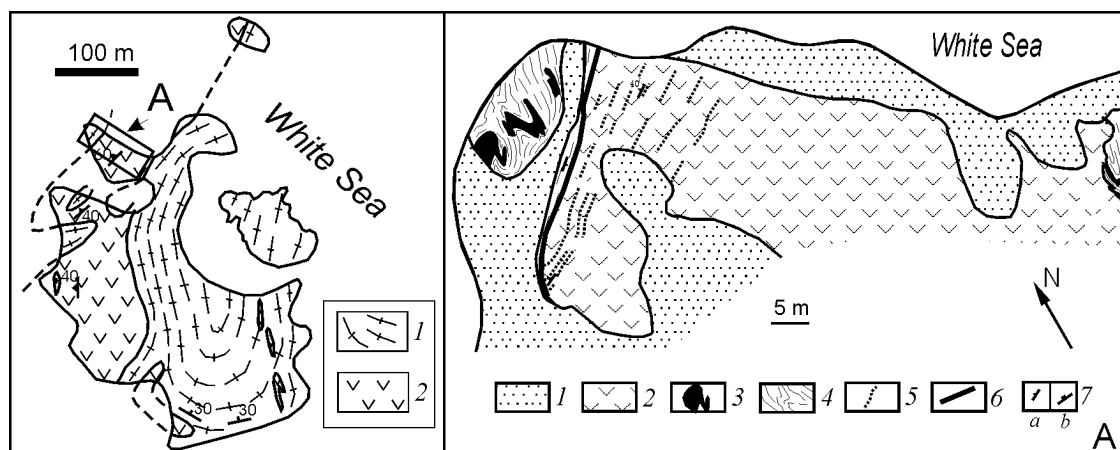


**Figure 11.** Geological map of Gorelyi Island, Kandalaksha Archipelago, White Sea (prepared by E. V. Sharkov and A. V. Chistyakov). 1 – Archean plagiomigmatites; 2 – drusite intrusion. A – Geological structure of the northern part of the drusite body. 1 – Quaternary deposits; 2 – plagioclase lherzolites, olivine and olivine-free gabbro-norites; 3 – garnet amphibolite bodies; 4 – gneisses and migmatites; 5 – primary layering; 6 – tectonic contact; 7 – strikes and dips of: (a) gneissosity, (b) primary layering.

Near the southeastern tip of the island, we found a small tectonic block of thinly layered and lenticularly layered rocks (alternating metapyroxenites and metagabbro-norites), analogous to those of Anisimov Island.

The gabbro-anorthosites of Voronii Island were dated at  $2460 \pm 10$  Ma (U–Pb zircon age), and pale rutile from these rocks has an age of  $1775 \pm 45$  Ma (T. B. Bayanova, personal communication), which coincides, within the error, with data on the Pezhostrov anorthosite massif and corresponds to the Karelian cycle.

The intrusion in Cape Tolstyik is located in the western shore of Kandalaksha Bay (Figure 3). This is a large lens-shaped body approximately 6 km long and 2 km wide, elongated northwestward. It is composed of gabbro-norites, gabbro-norite-anorthosites, and magnetite gabbro-norites, and gabbro-norite-diorites [Bogdanova, 1996; Efimov et al., 1987]. The intrusion was dated at  $2434 \pm 7$  Ma, the age of the host Archean plagiogneisses is  $2741 \pm 43$  Ma, and the cutting pink potassic granites have an age of  $2405 \pm 5$  Ma (U–Pb data on zircon; [Bibikova et al., 1993; Bogdanova, 1996]). The contacts of the body are tectonic. The rocks preserve their magmatic textures in the core of the intrusion and are transformed into garnet amphibolites and garnet–amphibole gneisses in the margins of the body and along crosscutting shear zones.

The intrusion is cut by at least three generations of mafic dikes. The earliest of them are roughly coeval with the intrusion itself, intermediate dikes are younger than the drusites but older than the potassic granites, and the youngest dikes cut the granites [Bogdanova, 1996]. According to Bogdanova [1996], the earliest dikes are compositionally close to the gabbro-norites of the massif, whereas the late dikes show similarities with the diorite derivatives. Analogous dikes were also found in the host rocks. The repeated magma injections (mafite bodies, dikes, and potassic granites) were associated with intense subhorizontal shearing and folding. According to S. V. Bogdanova, the rocks underwent then

metamorphic transformations with the development of high-pressure metamorphic mineral assemblages (predominantly garnet and hornblende) in the main body and two early dike generations, but not in the granites. The youngest mafic dikes predated regional deformations at 1.9–1.8 Ga [Alekshev et al., 1999].

#### Bodies of Ultramafic Rocks (Lherzolite–Gabbro-norite)

The lherzolite–gabbro-norite intrusions of Pezhostrov Island are a few relatively small bodies in the southern part of the island (Figure 4), which are hosted by the same Archean plagiomigmatites. In the Southern Body, 110 by 180 m in size, plagioclase lherzolites compose the western part and grade through olivine gabbro-norites to melanocratic norites in the eastern part (Figure 4a). This coarse layering is oriented generally conformably with the contacts. The rocks are mostly massive. The western contact of the body is tectonized, and its eastern contact is truncated by a younger migmatization zone 5–10 m thick, which abounds in angular rock fragments from the body that are transformed into amphibolites. Analogous migmatization zones and breccias, often having a pink color caused by potassic granites, occur at the contacts of the plagioclase olivine websterite body in Lodeinaya Bay (Figure 4b).

The intrusion of Gorelyi Island is elongated to the northeast (Figure 12) and has a length of approximately 1 km at a width of 300 m in the broadest part. Similarly to most of the intrusions described above, the initial sizes of the body are unknown, because it extends beneath the White Sea shoreline in the northeast and southwest and is truncated by a fault in the west. The eastern part of the body, which exhibits an intrusive contact with the host Archean gneisses (Figure 13), is composed of fine-grained massive rocks typical of inner-contact facies. The western

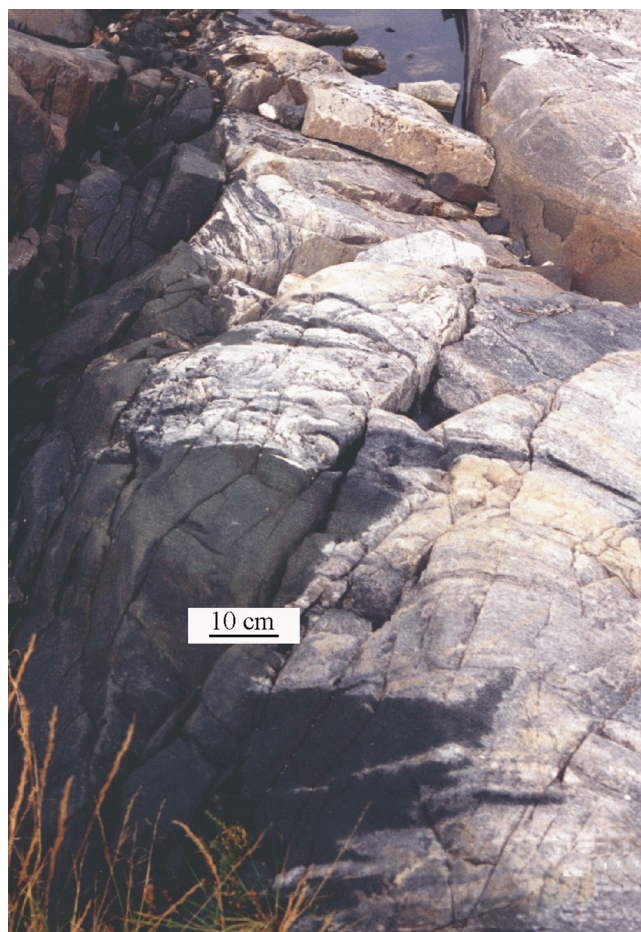


**Figure 12.** Character of contacts of the Gorelyi island lherzolite-gabbro-norite intrusion. Intrusive contact of the body (dark) with the host Archean plagiomigmatites (light gray in the right-hand part of the photo). The photo clearly demonstrates that apophyses of fine-grained gabbroids penetrate into the host rocks. Photo: A. V. Chistyakov.

part is layered, with alternating plagioclase lherzolite and olivine gabbro-norite layers from 30 to 50 cm thick, which are generally conformable with the trend of the body.

The drusite complex of Gorelyi Island shows two types of contacts. The primary intrusive contact with the host Archean granite-gneisses and plagiomigmatites has a complicated morphology with the extension of fine-grained inner-contact gabbroids into the host rocks along the migmatite banding and joints (Figure 13a). The rocks of these apophyses are usually amphibolized but may contain occasional relics of the primary fine-grained gabbro-norites with a gabbro-ophitic texture. The contact surface is almost vertical with minor deviations.

The western contact of the body is truncated by a younger migmatite zone (Figure 13b) and is characterized by the bending of the primary layering. This suggests that the body was still hot during its deformations (Figure 13). The rocks of the massif are transformed into amphibolite along the contact and are migmatized (impregnated migmatization).

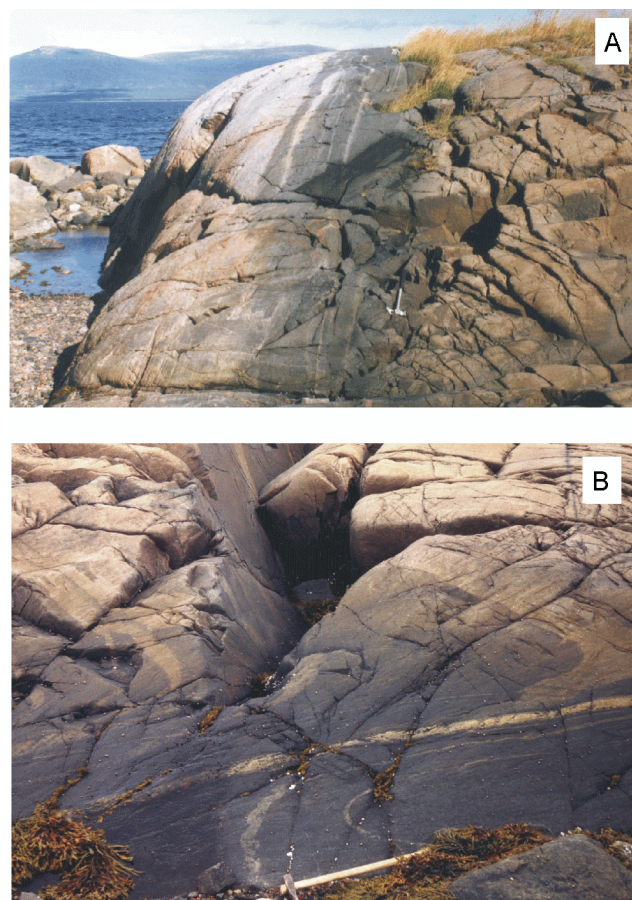


**Figure 13.** Western tectonic contact of the same body. Photo: A. V. Chistyakov. (A) General view of the contact: left—migmatites (light), right—olivine gabbro-norites. The migmatites and gabbro-norites are separated with an amphibolization zone affected by partial migmatization. (B) Bending of the primary layering along the tectonic contact zone. The bottom part of the photo demonstrates that the layered rocks are transformed into deformed blastomylonites (amphibolites). The detachment fault surface is marked by a vein of granitic material.

The lens-shaped body of fine-grained melanocratic metagabbro-norites in Lodeinyi Island is elongated to the northeast, conformably with the structure of the host gneisses and migmatites (Figure 5). This body is oriented obliquely relative to the roughly northern trend of the anorthosite body (see above). The intrusion was dated by B. V. Belyatskii (TIMS U-Pb zircon age) on a Finnigan MAT-261 eight-collector mass spectrometer at the Institute of Precambrian Geology and Geochronology, Russian Academy of Sciences, using our samples. The age of the intrusion was evaluated at  $2442 \pm 3.6$  Ma (Figure 14), i.e., roughly 10 m.y. younger than the age of the anorthosite bodies in Pezhostov and Voronii islands.

The primary intrusive contact of this body with the host Archean gneisses principally differs from the contact in Gorelyi Island. The former is marked by a specific rind,

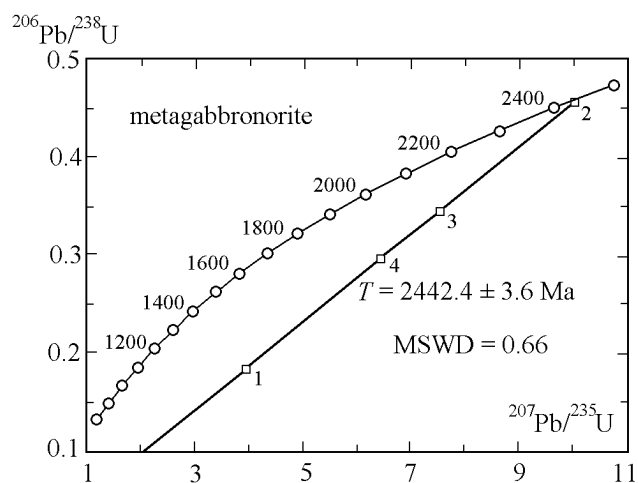


**Figure 14.** U–Pb zircon isotopic dating of the olivine gabbro intrusion in Lodeinyi Island. 1 – Zircon from the host hornfels and migmatite at 0.5 m from the contact; 2 – zircon from the central part of the “diffusion” contact zone; 3 – zircon from the inner-contact gabbro at 0.5 m from the contact; 4 – zircon from the olivine gabbro from the internal part of the body at 10 m from the contact.

approximately 1 m thick, which consists of green hornblende, clinopyroxene, plagioclase, and quartz and contains small (2–3 cm long) partially reworked skialiths of fine-grained gabbroids and host gneisses. The material of this rind grades, on the one hand, into gabbro and, on the other, into the host gneiss. The gneiss in the 1.5- to 2-m-thick outer-contact zone is partly recrystallized, its biotite decomposition gives rise to orthoclase, and the rock contains newly formed granophyric segregations and becomes more massive. These transformations were, perhaps,

caused by bimetasomatic processes, when the already solidified but still hot mafites interacted with the host granitic rocks in a manner resembling skarn processes. Obviously, the development of such a diffusion contact required that the host rocks were heated to higher temperatures than those at the “normal” intrusive contact, such as in Gorelyi Island.

The Yudom-Navolok and Shang intrusions (Figure 15) are exposed in the shores of Domashnyaya Bay, 200–250 km south of the Kandalaksha and Keret’ archipelagoes. In contrast to many other localities in the White Sea area (Belomorje), this one shows north-trending deformational structures that controlled the emplacement of intrusions of the drusite complex but did not experience intense metamorphic recycling [Stepanov, 1981].

The Yudom-Navolok intrusion is a relatively large body, which trends roughly northward for no less than 5 km and has a width from 80 to 150 m. It is composed of plagioclase lherzolites, pyroxenites, olivine gabbro, leucocratic gabbro, and granophyric gabbro and gabbro. The rare layering is oriented roughly to the north, conformably with the trend of the massif itself. Lherzolites are prone to be restricted to the southern exposures of the massif, which seem to correspond to its lower part.

The intrusive contacts with the host migmatized garnet-biotite gneisses are well exposed and can be observed in many outcrops. These contacts are commonly highly tortuous and complicated with apophyses and embayings, with the contact rocks abounding in xenoliths of the host rocks. The inner-contact zone is 3–5 m thick, consists of fine-grained gabbro, and is marked by xenoliths of garnet gneisses and amphibolites. The gabbro themselves always contain garnet and amphibole, mostly in the form of discontinuous rims around plagioclase and pyroxene grains or as inclusions in plagioclase.

A distinctive feature of the contact gabbro is the presence of granophyric varieties whose plagioclase laths are

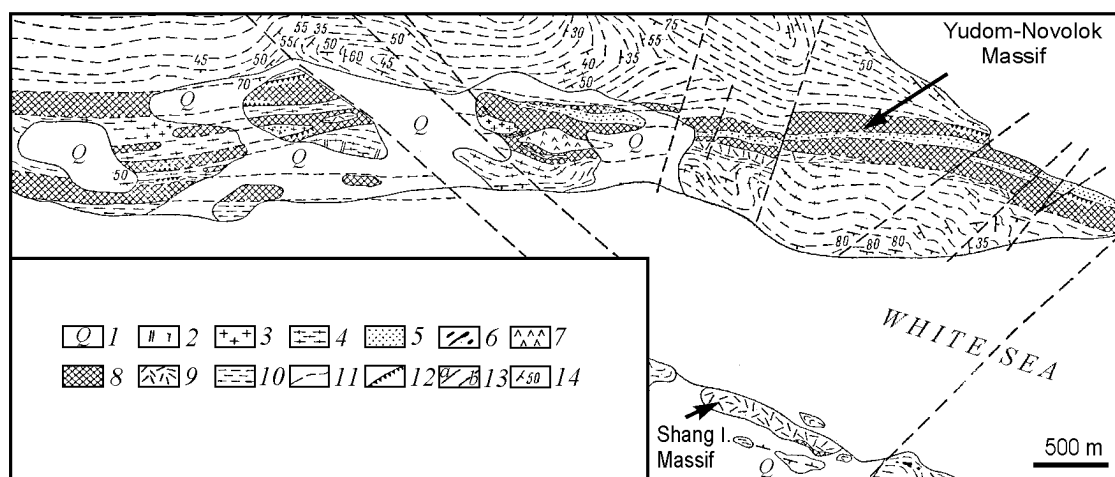


**Figure 15.** Schematic geological map of Domashnyaya Bay, White Sea (after [Stepanov, 1981]). 1 – Quaternary deposits; 2 – aplitic granites; 3 – pegmatoid granites; 4 – migmatization zones; 5 – hybrid rocks; 6 – metabasites; 7 – leucocratic gabbro; 8 – gabbro; 9 – plagioclase lherzolites; 10 – gneisses and migmatites; 11 – contacts of rocks; 12 – chilled contacts; 13 – faults: (a) confirmed, (b) inferred; 14 – dips of gneissosity and contacts.

**Table 1.** Composition (wt%) of olivine from rocks of the drusite complex

Sample	18(1)	18(2)	18(3)	18-1(1)	18-1(2)	704	705	V1	V7	P16	P30	P37
Rock	OP	OP	OP	OP	OP	L	OGN	L	L	L	ON	L
SiO <sub>2</sub>	37.63	36.92	37.65	38.19	37.87	37.90	37.51	36.67	37.07	37.87	38.08	37.61
FeO	24.29	25.64	24.7	27.47	27.39	22.55	24.03	18.74	25.29	20.25	20.70	21.95
MnO	0.17	0.19	0.14	0.40	0.37	0.34	0.21	0.23	0.21	0.27	0.25	0.28
MgO	38.41	37.89	38.07	35.39	35.65	38.83	37.5	42.3	36.93	42.68	41.06	39.45
NiO	0.43	0.34	0.45	0.27	0.25	0.28	0.58	0.65	0.59	0.38	0.50	0.57
Total	100.93	100.98	101.01	101.72	101.53	101.53	99.83	98.59	100.09	100.09	100.59	99.86
Fo	0.74	0.72	0.73	0.70	0.70	0.75	0.74	0.80	0.72	0.79	0.78	0.76

Note. Sampling sites: 18 and 18-1 – Anisimov Island; V1 and V7 – Voronii Island; 704 and 705 – Pezhostrov Island, Kandalaksha Bay, White Sea; P16/98 – Shang Island; P30/98 and P37/98 – Yudom-Navolok, Domashnyaya Bay, White Sea.

Rocks (in this table and below): L – lherzolite, OP – olivine pyroxenite (Ol + Opx±Cpx cumulate), PL – plagioclase lherzolite (Ol + Opx±Cpx±Pl), P – pyroxenite (Opx + Cpx), ON and OGN – olivine norite and gabbronorite (Opx + Cpx±Ol + Pl), GN – gabbronorite (Opx + Cpx + Pl), GA – gabronorite-anorthosite (Pl), GD – gabbrodiorite (Pl + Cpx±Opx + Mag).

armored with aggregates of quartz and orthoclase-perthite, with the amount of these aggregates attaining 15–20% of the rock by volume and sometimes making the gabbronorites granophyric. The outer parts of the body are cut by veinlets of granophyric granite a few dozen centimeters thick, with rectilinear parallel contacts. The composition and textures of these rocks are analogous to those of granites cutting the rocks of the layered series of the Burakovskii pluton in the Karelian craton [Bogina *et al.*, 2000]. In this context, it is worth noting that the rocks contain intercumulus granophyric quartz–orthoclase aggregates. As the intrusion crystallized, the segregation of this residual melt could produce crosscutting granophyric bodies, analogous to those in the Burakovskii pluton.

The chilled-zone gabbroids are cut by veinlets of fine-grained aplitic granite (up to 30–50 cm thick), which extend from the contact with the host gneisses and have undulating but sharp boundaries with small tongues. These veinlets of anatectic granites cut across the chilled facies of the intrusion and xenoliths. The granites commonly bear minor amounts (<5 vol%) of disseminated biotite and small aggregates of garnet grains.

The massif of Shang Island (1 km×100 m) is a homogeneous drusite body, consisting of massive lherzolites and plagioclase lherzolites. The contacts of the intrusion are concealed beneath the waters of the White Sea. Irregularly shaped lens-like gabbronorite bodies and rare thin segregations and veinlets of pegmatoid gabbronorites become more abundant in the northern shore of the island.

## Petrography of the Drusite Complex

The least altered rocks of the drusite complex are characterized by magmatic cumulative textures, because of which further descriptions will be given within the scope of terminology currently adopted for cumulate rocks. The chemistry of minerals (their microprobe analyses) are given in

Tables 1–5. The analyses were conducted at the Institute of Geology of Ore Deposits, Petrography, Mineralogy, and Geochemistry (IGEM), Russian Academy of Sciences, on a Cameca MS-46 microprobe at an accelerating voltage of 15 kV and a sample current of 50 nA. The counting time for each element was 70 s.

The following mineral symbols are used in the text below: olivine = Ol, orthopyroxene = Opx, clinopyroxene = Cpx (augite=Aug, pigeonite-augite = Pig-Aug), Cr-spinel = Chr, hornblende = Hbl, garnet = Grt, phlogopite = Phl, biotite = Bt, plagioclase = Pl, orthoclase = Or, quartz=Qtz, titanomagnetite = Ti-Mag, ilmenite = Ilm, apatite = Ap, zircon = Zr.

As can be seen from our data (Table 1), Ol has similar compositions in all Ol-bearing rocks. The composition of the orthopyroxene systematically decreases from En<sub>81</sub> to En<sub>63</sub> in the rock sequence from the lherzolites to gabbronorite-anorthosites (Table 2). It should be stressed that the pyroxene compositions (in both the magmatic assemblages and the reaction coronas) define fairly compact fields in a Wo–En–Fs diagram (Figure 16), which are somewhat shifted toward pigeonite-augite or ferrous hypersthene for some massifs.

Plagioclase lherzolites and lherzolites are the most widespread ultramafites of this complex, in which lherzolites are usually understood as a series of cumulates from Ol±Chr and Ol+Opx±Chr to Ol+Opx+Cpx±Chr. The intercumulus material can account for 30–35% of these rocks by volume. In the type-I cumulates, it is dominated by Pl and contains Opx and Aug; this material in the type-II cumulates also includes Opx and Aug, and the type-III cumulates contain plagioclase-dominated intercumulus material. Minor occasionally present minerals are Bt, Phl, Qtz, and rare Or and Ap. Formally, the petrography of these rocks corresponds to plagioclase lherzolite.

The mineral compositions vary within fairly broad ranges (mainly from intrusion to intrusion): olivine Fo<sub>79–80</sub>, orthopyroxene En<sub>78–80</sub>, clinopyroxene (augite) Wo<sub>43–46.5</sub>En<sub>47–49</sub>Fs<sub>8–10</sub>, and chromite contains 33–49.5 wt % Cr<sub>2</sub>O<sub>3</sub>; the interstitial plagioclase is An<sub>37–44</sub> and

**Table 2.** Composition (wt%) of pyroxenes from rocks of the drusite complex

no.	18-1(1)	18-1(2)	18-1(3)	18-1(4)	18(1)	18(2)	18(3)	18(4c)	18(4r)	18-7(1)	18-7(2)	18-7(3)
Rock	OP	OP	OP	OP	OP	OP	OP	OP	OP	OP	GN	GN
SiO <sub>2</sub>	52.18	51.99	52.22	56.01	52.07	51.77	51.77	54.79	53.59	54.15	51.24	51.13
TiO <sub>2</sub>	0.05	0.23	0.53	0.67	0.00	0.03	—	0.10	0.17	0.23	—	—
Al <sub>2</sub> O <sub>3</sub>	0.85	0.87	0.96	0.85	1.40	1.06	1.06	1.25	1.42	1.42	0.62	0.70
FeO	16.99	16.40	15.97	4.82	15.59	15.84	15.85	4.91	4.26	4.21	16.44	16.25
Cr <sub>2</sub> O <sub>3</sub>	—	—	—	0.60	0.07	—	—	0.66	0.37	0.77	—	—
MnO	0.39	0.35	0.37	0.15	0.19	0.15	0.15	0.04	0.03	0.06	0.18	0.15
NiO	—	—	0.05	0.05	—	0.08	0.08	0.05	0.06	0.06	0.09	0.08
MgO	29.32	28.82	28.8	16.27	29.43	29.27	29.22	16.02	15.46	15.75	29.70	29.73
CaO	0.22	1.67	1.20	20.86	0.22	0.17	0.17	23.14	23.58	23.98	0.43	0.24
Na <sub>2</sub> O	—	—	—	0.27	0.05	—	—	0.27	0.43	0.77	—	—
Total	100.00	100.33	100.10	100.55	99.02	98.37	98.30	101.23	99.37	101.40	98.70	98.28
Wo	0.4	3.0	2.2	44.0	0.4	0.3	0.3	46.9	48.7	48.7	0.8	0.4
En	74.7	73.1	74.2	47.8	76.6	76.3	76.3	45.2	44.4	44.5	75.5	76.0
Fs	24.9	23.8	23.6	8.2	23	23.4	23.4	7.8	6.9	6.8	23.7	23.5

no.	18-7(4)	18-7(5)	704-1	704-2	704-3	704-4	704-5	705-1	705-2	705-3	705(4)	707(1L)	707(1m)
Rock	GN	GN	L	L	L	L	L	OGN	OGN	OGN	OGN	GN	GN
SiO <sub>2</sub>	50.89	54.64	54.73	54.62	55.64	51.44	52.3	54.6	54.67	53.28	53.44	50.55	51.36
TiO <sub>2</sub>	—	0.22	0.12	0.13	0.09	0.17	0.29	0.07	0.11	0.08	0.36	—	0.28
Al <sub>2</sub> O <sub>3</sub>	0.89	3.04	2.03	1.97	1.57	3.23	3.58	1.34	0.99	2.59	2.50	1.03	1.94
FeO	17.14	4.49	10.04	11.08	9.17	7.13	6.24	13.37	14.89	6.72	5.71	29.23	10.9
Cr <sub>2</sub> O <sub>3</sub>	—	0.20	0.76	0.61	0.88	1.43	1.14	0.53	0.18	0.9	0.39	—	—
MnO	0.21	0.05	0.2	0.28	0.17	0.20	0.23	0.17	0.33	0.11	0.14	0.59	0.28
NiO	0.08	0.05	0.27	0.27	0.11	0.16	0.18	0.25	—	—	0.15	—	—
MgO	28.77	13.73	29.25	28.57	30.32	19.03	17.54	27.42	26.8	18.23	15.84	17.84	12.49
CaO	0.18	22.51	2.43	2.47	2.05	16.7	18.21	2.01	1.94	17.72	20.42	0.58	21.62
Na <sub>2</sub> O	—	1.23	0.15	—	—	0.51	0.27	0.12	—	0.37	0.95	0.06	0.97
Total	98.16	100.16	99.98	100.0	100.0	100.0	99.98	99.88	99.91	100.0	99.9	99.88	99.84
Wo	0.3	49.8	4.8	4.8	4.0	34.2	38.2	4.0	3.8	36.6	43.4	1.2	45.3
En	74.5	42.3	79.6	77.8	81.9	54.1	51.2	75.2	73.0	52.4	46.9	51.0	36.4
Fs	25.2	7.8	15.6	17.4	14.2	11.7	10.6	20.8	23.2	11.0	9.7	47.8	18.3

no.	707-2	707-3L	707-3m	707-4L	707-4m	707-5	708-1	708-2	708-3	708-4	708-5	708-6L
Rock	GN	GN	GN	GN	GN	GN	GN	GN	GN	GN	GN	GN
SiO <sub>2</sub>	51.10	50.55	52.36	52.86	51.66	51.76	51.67	53.05	52.27	51.82	51.87	49.70
TiO <sub>2</sub>	0.07	0.01	0.16	—	0.05	0.10	0.19	0.08	—	0.15	0.18	0.06
Al <sub>2</sub> O <sub>3</sub>	0.55	0.90	1.32	1.05	0.42	2.00	1.19	1.39	1.52	1.40	2.03	1.65
FeO	27.83	29.26	10.16	8.79	25.94	10.33	23.81	15.96	9.78	23.76	9.36	31.98
MnO	0.44	0.44	0.33	—	0.24	0.27	0.53	0.23	0.17	0.39	0.32	0.47
NiO	0.26	—	—	—	—	—	—	—	—	—	—	—
MgO	19.45	18.00	12.32	13.94	20.83	12.43	20.31	21.77	13.22	21.68	13.08	15.46
CaO	0.25	0.33	22.52	22.33	0.32	21.98	1.87	7.17	22.39	0.41	22.45	0.41
Na <sub>2</sub> O	—	0.42	0.66	0.57	0.22	0.84	0.23	0.18	0.44	0.36	0.61	0.20
Total	99.95	99.91	99.83	99.54	99.68	99.71	99.8	99.83	99.79	99.97	99.90	99.93
Wo	0.5	0.7	47.1	46.0	0.6	46.2	3.8	14.3	46.1	0.8	46.6	0.9
En	54.8	51.6	35.8	39.9	58.3	36.4	57.5	60.5	37.9	61.0	37.8	45.5
Fs	44.7	47.7	17.1	14.1	41.1	17.4	38.7	25.2	16.0	38.1	15.7	53.6

**Table 2.** Continued

no.	708-6m	708-7L	708-7m	Pzh8-1	Pzh8-2L	Pzh8-2m	V1	V7-1c	V7-1r	V7-2	V7-3	V8-1
Rock	GN	GN	GN	GN	GN	GN	L	L	L	L	L	P
SiO <sub>2</sub>	51.45	52.50	51.02	52.45	53.45	52.87	51.13	53.46	54.08	53.55	54.36	52.48
TiO <sub>2</sub>	0.20	0.02	0.05	–	0.15	–	0.20	0.20	0.28	0.18	0.33	0.33
Al <sub>2</sub> O <sub>3</sub>	1.93	1.50	0.89	0.98	1.32	0.70	3.57	3.14	3.04	3.04	2.89	2.91
FeO	11.41	9.86	28.51	25.78	9.32	25.71	6.00	6.38	5.11	5.98	4.67	5.61
Cr <sub>2</sub> O <sub>3</sub>	–	–	–	0.07	0.16	0.04	1.11	0.91	0.31	1.07	0.16	0.34
MnO	0.06	0.10	0.48	0.45	0.14	0.37	0.15	0.14	0.10	0.13	0.08	0.12
NiO	–	–	–	–	–	–	0.06	0.05	0.03	0.05	0.05	0.03
MgO	12.05	13.08	18.51	18.76	13.86	19.70	16.70	17.43	16.72	17.00	15.09	15.41
CaO	22.34	22.45	0.34	1.54	21.14	0.63	19.48	17.55	19.14	17.85	20.34	20.96
Na <sub>2</sub> O	0.48	0.39	0.17	–	0.59	–	0.80	0.98	1.11	0.98	0.92	1.08
Total	99.92	99.90	99.97	100.03	100.13	100.02	99.20	100.24	99.92	99.83	98.89	99.27
Wo	46.5	46.4	0.7	3.2	44.2	1.3	41.0	37.4	41.2	38.6	45.2	44.7
En	34.9	37.6	52.9	54.2	40.3	56.6	48.9	51.7	50.1	51.1	46.6	45.7
Fs	18.6	16.1	46.4	42.6	15.4	42.1	10.1	10.9	8.8	10.3	8.2	9.5
no.	V8-2	V8-3	V8-4	Lod-1	Lod-2	P16-1k	P16-2	P16-2	P30-c	P30-r		
Rock	P	P	P	GN	GN	L	L	L	ON	ON		
SiO <sub>2</sub>	53.95	52.86	52.78	53.15	53.50	53.86	52.37	50.68	52.87	52.09		
TiO <sub>2</sub>	0.25	0.28	0.12	0.12	–	–	0.13	0.32	0.08	0.50		
Al <sub>2</sub> O <sub>3</sub>	2.80	3.04	2.63	1.79	1.14	0.85	3.14	4.48	1.36	1.79		
FeO	5.62	5.88	13.65	17.83	18.60	12.14	4.94	5.26	12.38	13.93		
Cr <sub>2</sub> O <sub>3</sub>	0.16	0.32	1.37	–	–	–	0.94	1.04	0.45	0.19		
MnO	0.14	0.06	0.27	0.20	0.18	0.27	0.06	0.12	0.21	0.25		
NiO	–	0.05	0.06	–	–	0.09	–	–	0.08	0.10		
MgO	15.89	16.53	23.02	26.14	24.89	31.18	17.81	13.98	29.29	28.62		
CaO	20.83	19.55	5.65	0.62	1.62	0.29	18.12	20.89	2.49	1.89		
Na <sub>2</sub> O	0.73	0.88	0.19	0.14	0.08	–	1.05	1.46	–	–		
Total	100.37	99.45	99.74	99.99	100.01	98.68	98.56	98.23	99.21	99.36		
Wo	43.9	41.4	11.6	1.2	3.2	0.5	38.7	46.9	4.7	3.6		
En	46.6	48.7	66.0	71.2	68.0	81.3	52.9	43.7	77.0	75.4		
Fs	9.5	9.8	22.4	27.6	28.8	18.2	8.3	9.4	18.3	21.0		
no.	P30-r	P37-1	p37-1k	P37-3	P37-4k	t-1-1	t-1-2	t-2-1L	t-2-1m			
Rock	ON	L	L	L	L	GN	GN	GD	GD			
SiO <sub>2</sub>	52.77	53.50	52.84	53.76	52.69	53.54	52.39	49.02	51.94			
TiO <sub>2</sub>	–	0.10	0.22	0.23	–	–	1.31	–	0.24			
Al <sub>2</sub> O <sub>3</sub>	2.61	1.27	3.21	2.97	1.76	1.50	2.13	0.70	2.03			
FeO	14.76	11.36	4.22	5.33	13.53	16.11	4.74	35.49	13.20			
Cr <sub>2</sub> O <sub>3</sub>	0.12	0.42	0.91	0.56	–	–	–	–	–			
MnO	0.28	0.22	0.12	0.13	0.25	0.27	0.09	0.59	0.06			
NiO	0.08	0.06	0.06	0.09	0.06	–	–	–	–			
MgO	28.44	30.28	15.19	17.00	29.77	25.80	15.22	13.65	10.21			
CaO	0.62	2.38	22.43	20.30	0.32	2.58	23.60	0.39	21.32			
Na <sub>2</sub> O	–	0.28	1.16	1.01	–	–	0.49	0.11	0.94			
Total	99.68	99.87	100.36	101.38	98.38	99.80	99.97	99.97	99.94			
Wo	3.6	4.4	47.8	42.1	0.6	5.0	48.6	0.8	46.5			
En	75.7	78.7	45.0	49.1	78.9	70.0	43.6	39.9	31.0			
Fs	20.7	16.9	7.2	8.8	20.5	24.9	7.8	59.2	22.6			

Note. Sampling sites: 18-1/1, 18-1, and 18-7 – Anisimov Island; V1, V7, and V8 – Voronii Island; Lod1 and Lod2 – Lodeinyi Island; 704, 705, 707, 708, and Pzh8 – Pezhostrov Island; t1, t2, t3, and t4 – Cape Tolstik (all are in Kandalaksha Bay of the White sea); P16/98 – Shang Island; P30/98 and P37/98 – Yudom-Navolok, Domashnyaya Bay, White Sea.

In the line with no., sample numbers are supplemented with the following indices denoting the grain or grain part examined: c – grain core, r – grain rim; in the presence of exsolution textures, L – lamella (lamellae), m – matrix, k – drusite corona. Here and below, dashes mean contents below the detection limit.

**Table 3.** Composition (wt%) of Cr-spinel from rocks of the drusite complex

Sample	V1-1	V1-2	V1-3	V1-4	V1-5	V1-6	V8	704	705-1	705-2	P16-1	P16-2
Rock	L	L	L	L	L	L	P	L	OGN	OGN	L	L
TiO <sub>2</sub>	0.93	2.99	0.87	0.48	0.55	0.47	0.40	0.03	0.42	0.70	–	–
Al <sub>2</sub> O <sub>3</sub>	19.12	14.57	18.78	20.48	19.80	17.50	15.55	15.72	20.61	16.78	43.25	40.66
FeO	43.59	45.32	39.64	27.63	27.58	27.70	28.24	29.8	33.2	33.6	24.96	25.68
MnO	0.09	0.10	0.08	–	–	0.39	0.04	0.40	0.35	0.39	–	–
Cr <sub>2</sub> O <sub>3</sub>	33.73	35.27	36.96	45.41	43.72	48.77	49.52	46.86	40.10	43.55	22.77	25.42
MgO	2.53	2.22	2.94	6.7	6.63	5.92	5.07	5.66	3.79	3.97	9.14	9.2
NiO	0.20	0.27	0.13	0.14	0.14	0.13	0.08	0.24	0.55	0.06	0.17	0.09
V <sub>2</sub> O <sub>5</sub>	0.84	0.57	0.34	0.39	0.37	0.36	0.41	0.45	0.32	0.32	–	–
ZnO	0.06	0.06	0.12	0.14	0.1	0.21	0.42	–	–	–	0.20	0.17
Total	101.09	101.37	99.86	101.40	98.92	101.45	99.73	99.16	99.34	99.37	100.49	101.22
Al	0.74	0.58	0.74	0.77	0.77	0.67	0.62	0.62	0.81	0.67	1.47	1.38
Cr	0.88	0.94	0.98	1.15	1.13	1.26	1.31	1.24	1.05	1.16	0.52	0.58
Fe <sup>3+</sup>	0.34	0.33	0.24	0.06	0.07	0.05	0.05	0.14	0.12	0.14	0.01	0.04

Note. See Table 2 for sampling sites.

the pigeonite–augite has the composition  $Wo_{34}En_{54}Fs_{12}$ . The dark mica (up to 5–7 vol %) is mostly biotite or, more rarely, phlogopite with  $Mg/Fe > 2$  (Table 4).

The interstitial plagioclase of these rocks usually has a dark color due to very fine dust of aluminous spinel, as was determined on a microprobe [Larikova, 2000]. Larikova believes that the spinel was produced via the metamorphic decomposition of the anorthite component of plagioclase.

The olivine gabbronorites differ from the rocks described above in bearing cumulative plagioclase, which occurs as weakly zonal dusted labradorite laths ( $An_{55-68}$  in the cores). The orthopyroxene ( $Wo_4En_{73-75}Fs_{21-23}$  of these rocks is less magnesian than in the plagioclase lherzolites, whereas the composition of olivine does not vary. The intercumulus pigeonite–augite is  $Wo_{36}En_{53}Fs_{11}$  and accounts for 25% of

the rocks by volume. The potassic feldspar ( $Or_{93}$ ), Qtz, Bt, and Ilm occur as volumetrically subordinate intercumulus phases.

The pyroxenites, melanocratic norites, and melanocratic gabbronorites usually consist of orthopyroxene, more rarely of orthopyroxene–clinopyroxene cumulates, sometimes with minor olivine amounts. The orthopyroxene is bronzite ( $Wo_{3-5}En_{76-78}Fs_{20-27}$ ). The clinopyroxene commonly contains exsolution lamellae of broadly varying composition (Table 2). The intercumulus usually contains alkaline feldspar, whose composition varies from K–Na varieties to nearly pure orthoclase (Table 5, analyses 705, 707, and 708).

The norites and gabbronorites are plagioclase–orthopyroxene and plagioclase–orthopyroxene–clinopyroxene cumulates, whose orthopyroxene is bronzite ( $Wo_1En_{75}Fs_{24}$ )

**Table 4.** Composition (wt%) of biotite from rocks of the drusite complex

Sample	P16	P30	P37	705	708	707	V1-1	V1-2	V7-1	V7-2	V8
Rock	L	ON	L	OGN	GN	GN	L	L	L	L	P
SiO <sub>2</sub>	38.68	38.32	38.85	38.99	37.58	38.94	38.94	38.14	39.73	40.52	39.58
TiO <sub>2</sub>	4.27	7.62	6.64	7.05	4.59	5.41	7.19	5.04	6.12	5.79	5.49
Al <sub>2</sub> O <sub>3</sub>	16.04	15.08	15.74	14.06	15.74	14.90	16.48	15.89	16.08	15.42	14.91
Cr <sub>2</sub> O <sub>3</sub>	0.63	0.48	0.34	0.11	n.d.	n.d.	0.20	0.12	0.16	0.25	0.29
FeO	6.20	8.75	8.32	14.56	18.94	14.94	9.56	9.13	8.26	7.26	6.90
MnO	–	–	–	–	0.11	0.04	–	–	–	–	–
MgO	19.29	16.70	16.5	14.66	12.32	15.49	16.33	16.73	17.66	19.45	19.04
CaO	–	–	0.11	–	–	–	–	–	–	–	–
K <sub>2</sub> O	9.48	9.29	9.60	10.00	9.90	9.85	9.54	9.71	9.43	9.56	9.71
Na <sub>2</sub> O	0.44	0.35	0.15	0.35	0.42	0.42	0.24	0.22	0.39	0.42	0.19
NiO	0.22	0.25	0.43	n.d.	n.d.	n.d.	0.18	0.17	0.17	0.18	0.22
Total	95.25	96.84	96.68	99.78	99.61	99.99	98.66	95.15	98.00	98.85	96.33
Mg/Fe	2.41	1.48	1.54	0.50	0.80	0.74	1.33	1.42	1.66	2.08	2.14

Note. See Table 2 for sampling sites; n.d. – not determined.

**Table 5.** Composition (wt%) of feldspars from rocks of the drusite complex

Sample	18-7(1)	18-7(2)	704-1	704-2	705-1	705-2	707-1	707-2	707-3	707-5	708-3	708-4
Rock	GN	GN	L	L	OGN	OGN	GN	GN	GN	GN	GN	GN
SiO <sub>2</sub>	59.11	54.23	55.63	56.16	56.99	65.27	55.22	56.20	59.62	63.30	52.77	53.70
Al <sub>2</sub> O <sub>3</sub>	24.85	27.45	29.53	27.17	26.52	17.73	27.93	27.36	25.02	18.37	29.57	29.32
FeO	—	—	0.49	0.35	—	0.08	0.12	0.25	0.25	0.38	—	0.07
CaO	6.32	10.55	7.39	9.53	9.02	0.06	10.77	9.33	7.14	0.14	12.73	12.11
Na <sub>2</sub> O	8.07	6.13	6.60	6.27	7.06	0.81	5.79	6.41	7.65	0.54	4.33	4.58
K <sub>2</sub> O	0.06	0.05	0.28	0.20	0.08	15.95	0.10	0.22	0.12	15.36	0.3	0.15
Total	98.41	98.41	99.92	99.68	99.68	99.90	99.93	99.77	99.80	98.09	99.7	99.93
Or	0.3	0.3	1.7	1.1	0.4	92.5	0.6	1.2	0.7	94.3	1.7	0.9
Ab	69.5	51.1	60.7	53.7	58.4	7.2	49	54.7	65.5	5.0	37.5	40.3
An	30.1	48.6	37.6	45.1	41.2	0.3	50.4	44	33.8	0.7	60.8	58.8

Sample	708-5	708-6	708-7	708-8	708-9	V1-1(1)	V1-1(2)	V1-1(3)	V1-2	V1-3c	V1-3r	V8-1c
Rock	GN	GN	GN	GN	GN	L	L	L	L	L	L	P
SiO <sub>2</sub>	54.59	54.63	54.86	55.6	63.52	63.02	65.59	64.69	53.44	51.26	53.59	53.33
Al <sub>2</sub> O <sub>3</sub>	28.3	28.35	28.16	27.88	18.08	22.31	21.88	18.44	29.23	32.01	30.36	28.23
FeO	0.04	0.11	0.03	0.28	0.34	0.05	0.04	0.03	2.86	0.10	2.23	1.30
CaO	11.44	11.13	11.20	10.59	0.20	5.05	2.36	0.36	5.72	12.26	7.33	8.26
Na <sub>2</sub> O	5.25	5.47	5.47	5.43	0.79	8.28	10.39	3.05	6.96	3.65	6.04	5.53
K <sub>2</sub> O	0.19	0.23	0.35	0.11	15.48	0.43	0.42	11.47	0.23	0.11	0.22	0.17
Total	99.81	99.92	100.07	99.89	98.41	99.14	100.68	98.04	98.44	99.39	99.77	96.82
Or	1.1	1.3	1.9	0.6	91.9	2.5	2.3	69.9	1.5	0.7	1.4	1.1
Ab	44.9	46.5	46.0	47.8	7.1	72.9	86.8	28.3	67.8	34.8	59.0	54.2
An	54.0	52.3	52.1	51.5	1.0	24.6	10.9	1.8	30.8	64.5	39.6	44.7

Sample	V8-1r	V8-2	V8-3	P30c	P30r	P37-1	P37-2	764-11	764-12	t-1	t-2	t-3	t-4
Rock	P	P	P	ON	ON	L	L	GD	GD	GD	GD	GD	GD
SiO <sub>2</sub>	54.10	51.60	54.42	64.46	65.74	64.86	58.19	59.64	62.82	51.03	50.98	62.34	61.38
Al <sub>2</sub> O <sub>3</sub>	28.13	30.91	28.81	19.35	19.8	22.54	26.19	24.34	22.85	30.97	31.23	23.71	23.74
FeO	1.03	1.78	—	0.05	0.04	0.10	0.10	0.05	0.08	—	—	0.27	0.86
CaO	8.30	8.58	9.00	1.23	0.56	1.15	6.67	7.18	4.53	14.00	13.58	4.80	5.32
Na <sub>2</sub> O	6.48	5.47	6.34	4.02	2.82	9.89	7.78	7.21	8.49	3.51	3.95	8.48	8.28
K <sub>2</sub> O	0.13	0.14	0.14	9.37	11.11	0.83	0.19	0.63	0.50	0.15	0.13	0.27	0.24
Total	98.17	98.48	98.72	98.48	100.07	99.37	99.12	99.05	99.27	99.66	99.87	99.87	99.82
Or	0.8	0.9	0.8	56.8	70.0	5.0	1.1	3.6	2.9	0.9	0.7	1.6	1.4
Ab	58.1	53.1	55.6	37.0	27.0	89.3	67.1	62.2	75.0	30.9	34.2	75.0	72.8
An	41.1	46.0	43.6	6.3	3.0	5.7	31.8	34.2	22.1	68.2	65.0	23.4	25.8

Note. See Table 2 for sampling sites; sample 764 is gabbro-diorite from Cape Tolstik (from [Bogdanova, 1996]).

or interstitial pigeonite (the composition of the matrix and lamellae is, respectively,  $Wo_1En_{53}Fs_{46}$  and  $Wo_{26}En_{38}Fs_{16}$ ); the clinopyroxene is augite ( $Wo_1En_{52}Fs_{47}$ ), and the plagioclase has the composition  $An_{52-60}$ .

The gabbro-norites-anorthosites and anorthosites are plagioclase cumulates, usually having coarse-grained textures. For example, anorthosites in the Northern Massif of Pezhostrov Island are dominated (75–95%) by subhedral cumulus plagioclase ( $An_{65-73}$ ) slightly clouded by tiny inclusions of ore minerals. The inter-

cumulus minerals include four distinct pyroxene types: (1) partly inverted Pig ( $Wo_{14}En_{62}Fs_{24}$ ) with micrographic exsolution textures (Figure 17) or inverted Pig with coarse clinopyroxene ( $Wo_{45-46}En_{38-40}Fs_{15-16}$ ) lamellae parallel to (001) in an orthopyroxene matrix ( $Wo_1En_{53-56}Fs_{41-46}$ ); (2) inverted Pig-Aug with analogously oriented coarse orthopyroxene lamellae ( $Wo_1En_{45}Fs_{54}$ ) in clinopyroxene ( $Wo_{46-47}En_{35-38}Fs_{16-19}$ ); (3) more rare Opx ( $Wo_{3-4}En_{55-58}Fs_{38-42}$ ) with thin Cpx ( $Wo_{45-46}En_{38-40}Fs_{15-16}$ ) lamellae parallel to (100);

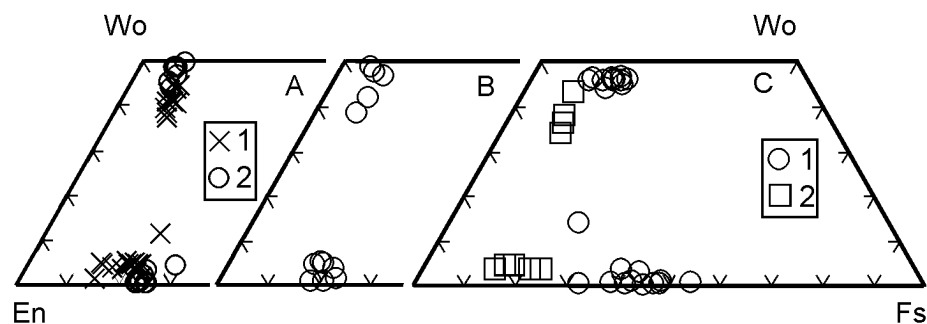


**Figure 16.** Composition of pyroxenes in rocks of the drusite complex. A – (1) Voronii Island, (2) Anisimov Island; B – Yudom-Navolok and Shang Island intrusions; C – Pezhostrov intrusion: (1) Southern Massif, (2) Northern Massif.

and (4) rare Aug ( $Wo_{45-46}En_{36-37}Fs_{17-18}$ ) with Opx ( $Wo_1En_{45}Fs_{54}$ ) lamellae. Both the plagioclase and the pyroxene usually show broad compositional variations even within a single hand-specimen. The compositional variability, the complete breakdown of the pigeonite solid solution, and the graphical exsolution textures suggest that the crystallization rate was high. Other intercumulus minerals are Bt, Qtz, Ort, Ilm, Ti-Mag, Ap, and Zr.

The magnetite gabbronorites and gabbro diorites were examined in the Tolstik Massif, in which they occur together with gabbronorites and anorthosites. These rocks are quite rich in titanomagnetites (up to 7–10 vol %). The relict minerals are inverted Pig and Pig-Aug and Pl ( $An_{23-24}$ ).

The compositions of minerals and rocks in massifs of the drusite complex and large layered plutons in the Baltic Shield are practically identical. The cumulus assemblages

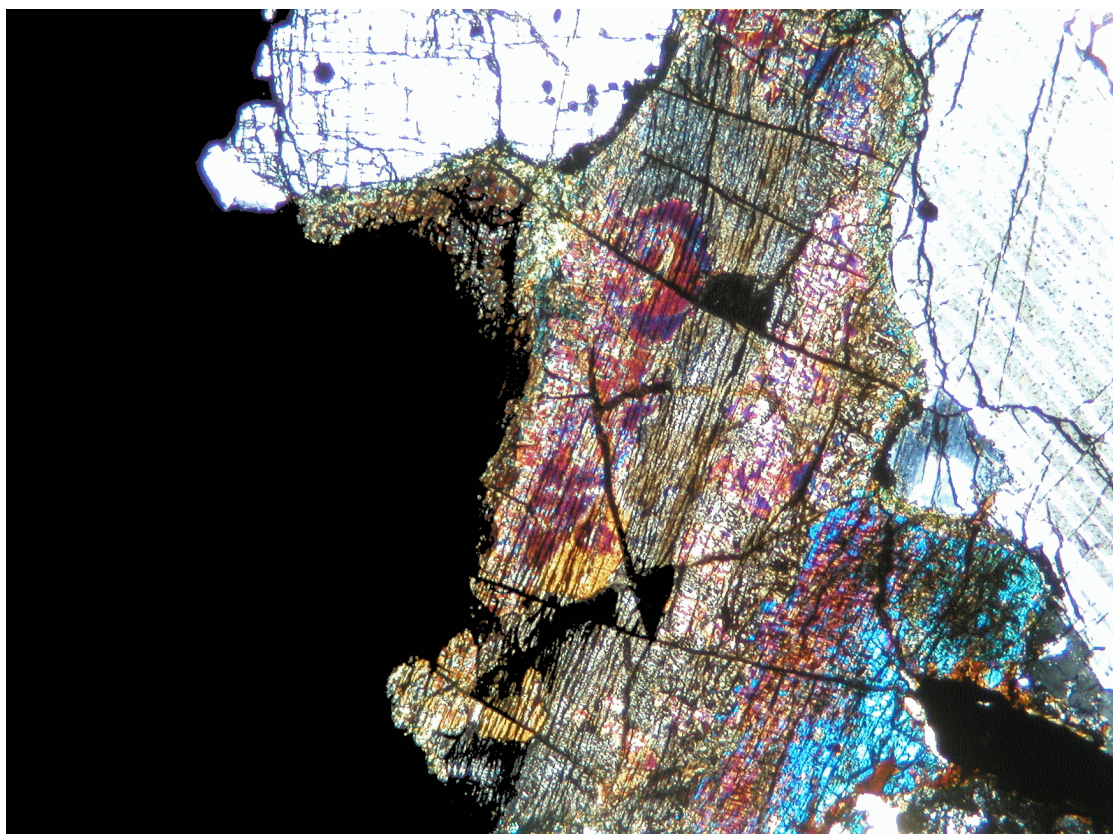


**Figure 17.** Partly decomposed pigeonite grain with graphical exsolution textures. Gabbronorite from the Yudom-Navolok intrusion, petrographic thin section, magnification 12 $\times$ , crossed polarizers.

**Table 6.** Composition of chilled margins and dikes of different Drusite (coronite) intrusions

Sample location	1	2	3	4	5	6	7	8	9	10	11	12	13	14	15	16	17
SiO <sub>2</sub>	51.20	51.90	52.80	51.72	51.52	53.27	51.85	50.06	55.56	48.91	44.82	53.82	53.25	50.20	49.94	53.80	53.90
TiO <sub>2</sub>	0.97	0.45	0.52	0.25	0.50	0.53	0.40	1.12	0.49	1.02	0.58	0.63	0.83	0.51	0.66	0.80	0.83
Al <sub>2</sub> O <sub>3</sub>	15.40	14.90	15.60	16.57	15.34	15.32	17.65	14.13	13.30	14.71	5.15	16.26	7.40	12.57	11.27	12.70	15.00
Fe <sub>2</sub> O <sub>3</sub>	1.61	1.78	0.68	0.96	2.18	1.79	0.33	13.86	1.62	2.97	1.49	0.25	0.75	1.00	0.73	0.93	0.78
FeO	10.00	8.28	8.38	6.32	7.04	7.76	7.62	—	7.90	9.66	14.43	7.73	8.73	9.74	9.68	9.24	7.18
MnO	0.16	0.14	0.15	0.16	0.10	0.19	0.14	0.19	0.18	0.19	0.26	0.16	0.18	0.16	0.17	0.16	0.15
MgO	8.66	8.63	7.99	9.04	7.68	7.46	7.12	6.73	7.46	5.68	24.09	7.53	13.19	14.31	15.98	9.11	9.19
CaO	7.44	7.70	9.68	12.40	11.76	9.61	10.30	10.53	8.99	9.93	4.83	9.05	12.49	8.64	7.97	8.66	8.31
Na <sub>2</sub> O	2.77	3.78	3.08	2.07	2.16	2.34	2.00	2.10	2.26	3.83	0.66	2.70	1.97	1.67	1.61	2.54	2.53
K <sub>2</sub> O	0.49	0.80	0.31	no	0.48	0.48	0.58	0.23	1.16	1.16	0.18	0.56	0.52	0.53	0.56	1.28	1.02
P <sub>2</sub> O <sub>5</sub>	0.12	0.12	0.10	0.05	—	0.15	0.11	0.10	0.04	0.12	0.09	0.24	—	—	0.09	0.13	0.12
Cr <sub>2</sub> O <sub>3</sub>	0.02	0.06	0.04	0.03	—	0.02	—	—	—	—	—	—	—	—	—	—	—
BaO	0.02	—	—	—	—	0.04	0.06	—	—	—	0.03	0.06	—	—	—	—	—
S	—	0.06	0.02	0.12	—	0.02	0.02	—	—	—	0.02	<0.02	—	—	—	—	—
LOI	0.85	0.97	0.71	0.71	1.24	0.58	1.41	—	—	—	2.96	1.06	0.09	0.96	1.25	1.02	0.93
Total	100.00	100.00	100.00	100.39	100.00	99.50	99.50	99.60	100.07	99.62	99.59	100.07	99.40	100.29	99.92	100.37	99.94
V	108	119	52	131	—	—	—	—	—	—	—	—	—	—	—	—	—
Cu	—	2730	850	no	—	—	—	—	—	—	—	—	—	—	—	—	—
Ni	170	190	150	133	—	—	—	—	—	—	—	—	—	—	—	—	—
Co	63	47	<40	55	—	—	—	—	—	—	—	—	—	—	—	—	—

Note. Gabbro-anorthosite massifs: Samples 1–3 – Northern Pezhostrovsky massif (1 – chilled margin, 2 – xenolith of porphyritic thin-grained gabbro (hyperstene porphyrite), 3 – dike of garnet amphibolite), 4 – chilled margin of the Boyarskiy massif, northern Karelia; 5–7 – Voronyi Island massif (5 – chilled margin, 6 – dike of garnet amphibolite, 7 – garnet amphibolites upon volcanics with relict volcanic structures); 8–10 – mafic dikes from the Tolstic massif (8 – I type, 9 – II type, 10 – III type); 11–12 – dikes of the Anisimov Island massif (11 – metaperidotite, 12 – garnet amphibolite). Lherzolite-gabbro massifs, chilled margins: 13 – Gorelyi Isl.; 14 – Chupa; 15 – Malye Salnye Tundras; 16 – Lodeinyi Island; 17 – Yudom-Navolok. Sources: 1–3 – after [Sharkov *et al.*, 1994]; 4 – after [Stepanov, 1981]; 8–10 – after [Bogdanova, 1996]; 14–15 – after [Malov and Sharkov, 1978]; samples 5–7, 11–13 and 16–17 were analyzed in the IGE M RAS.

are always of two major types: (1) ultramafic cumulates (Ol±Chr, Ol+Opx±Chr, Ol+Opx+Cpx±Chr, Opx±Cpx, Opx+Pl±Ol, and Opx+Cpx+Pl±Ol), which are typical of the lower portions of the intrusions; and (2) mafic cumulates (Opx+Pl±Cpx, Pl, and Pig+Pg-Aug+Pl±Mgt), which compose the upper parts of the intrusions. However, while all of these rocks in the plutons make up a single body, they occur in the drusite complex as arrays of small individual bodies with the corresponding compositions of their inner-contact zones (Table 6), so that they can be considered as if collectively composing a large layered intrusion “eparated” into fractions.

In contrast to the cumulates of layered plutons, the rocks of the drusite complex usually have elevated contents of intercumulus material (up to 25–35 vol %). In large layered intrusions, analogous contents of the intercumulus material are characteristic only of rocks in the marginal parts [Sharkov, 1980]. Considered together with the aforementioned variability of the chemistry of minerals, their zonal character, and the often incomplete exsolution of the pigeonite pyroxene, these facts suggest that coronite gabbro bodies were small in size and solidified in a regime typical of the marginal zones of large intrusions.

The rocks of some massifs of the drusite complex (anorthosites in the massifs of Pezhostrov and Voronii islands, in the lherzolite massif in Gorelyi Island, and others) occasionally contain angular xenoliths of porphyritic metagabbro. Judging from the results of their studying in rocks from the Pezhostrov Massif, these rocks are fragments of the material composing the feeders of the intrusions [Sharkov et al., 1994].

### Coronite Textures in the Rocks of the Complex

Grain boundaries between plagioclase and mafic minerals are marked by newly formed rims of fine-grained metamorphic minerals: Opx, Cpx, Grt, and green Hbl. These rims were formed in at least two stages. The earliest of them are concentrically zoned rims along the boundaries of olivine and plagioclase grains. Their inner (near olivine) parts consist of columnar Opx grains, and the outer portions are made up of columnar Cpx (diopside) crystals with tiny “lashes” of spinel (Figure 18). The coronite rims have roughly constant thicknesses and are often 1.5–2 times thicker than the olivine grains enclosed in them. In places, for example, in the rocks of the Shang-island intrusion, these rims account for 15–20% (or even more) of the rock by volume, with patches consisting entirely of a mosaic of adjacent rounded concentrically zoned ortho- and clinopyroxene coronas that are completely devoid of olivine and plagioclase. These textures are commonly thought to have been produced by the reaction between magnesian olivine and calcic plagioclase at  $T = 1000\text{--}1100^\circ\text{C}$  and  $P = 8 \pm 2$  kbar [Green and Hibberson, 1970].

The outer parts of these textures are preserved only occasionally and are commonly replaced by younger fine-grained clinopyroxene–garnet–amphibole aggregates of metamorphic genesis [Larikova, 2000]. Analogous rims, composing younger coronite textures, widely develop along grain boundaries of

mafic and ore minerals with plagioclase [Korikovskiy, 2004] and are most typical of gabbroids (Figure 18b).

It is worth noting that the coronite textures in intrusions of the drusite complex develop unevenly. In some of the youngest plagioclase lherzolite bodies in Pezhostrov and Shang islands and in the Yudom-Navolok rocks, coronas develop only along contacts between olivine and plagioclase but are absent at contacts between pyroxenes and plagioclase (Figure 18a). Conceivably, this can be explained by the fact that these massifs were not affected by intense metamorphic reworking due to their distant position from the Svecofennian Main Lapland Fault (see below).

### Geochemistry

The contents of major, trace, and rare-earth elements in the rocks of the intrusions are presented in Tables 6–9. All analyses were conducted at the Institute of Geology of Ore Deposits, Petrography, Mineralogy, and Geochemistry (IGEM), Russian Academy of Sciences. The rocks were analyzed for major elements by conventional techniques of wet chemistry. Trace and rare elements were determined by XRF on a PW 2400 (Philips) X-ray spectrometer, and REE were analyzed by ICP-MS on a PlasmaQuad PQ2 + Turbo (VG Instruments) quadrupole mass spectrometer at the Central Chemical laboratory of the same institute.

The whole rock series is classified as highly magnesian, with MgO contents attaining 27 wt%. Most of the rocks are low-Ti ( $\text{TiO}_2 < 1$  wt%) and low- to moderate-Al ( $\text{Al}_2\text{O}_3 < 15$  wt%), except only for the gabbroanorthosite and anorthosite members of the complex, whose  $\text{Al}_2\text{O}_3$  contents are as high as 20–27 wt%. The rocks exhibit relatively broad variations in the  $\text{SiO}_2$  contents (up to 54 wt%), and some of them contain Qtz or are Qtz-normative.

Figures 19 and 20 demonstrate the contents of some major and minor elements in the rocks in correlation with the MgO contents. The chemical variations within small and quite homogeneous bodies are insignificant, but the chemistry of the rocks notably varies from massif to massif. As can be seen from Figure 19, rock compositions of the drusite complex generally display the same relations as in the Burakovsky layered pluton. Some differences exist only in the distribution of aluminum and calcium: the rocks containing from 10 to 30 wt% MgO include less aluminous and more calcic varieties, such as metasomatic clinopyroxenites, and this affects the configuration of the corresponding compositional fields.

It is worth noting that the REE patterns (Figure 21) are absolutely analogous for all rock types within individual bodies and for all massifs as a whole, which testifies for the homogeneity of the parental magmas of all intrusions in the complex. The Eu anomalies are weak (if any) and are controlled by the plagioclase concentrations in the rocks. The rocks of the complex are typically enriched in LREE, with Ce/Yb as high as 5.65 and flat patterns over HREE. As can be seen from Figure 21, the REE patterns of the rocks practically completely overlap with the fields for rocks composing the layered series of the Burakovsky pluton. Both fields com-

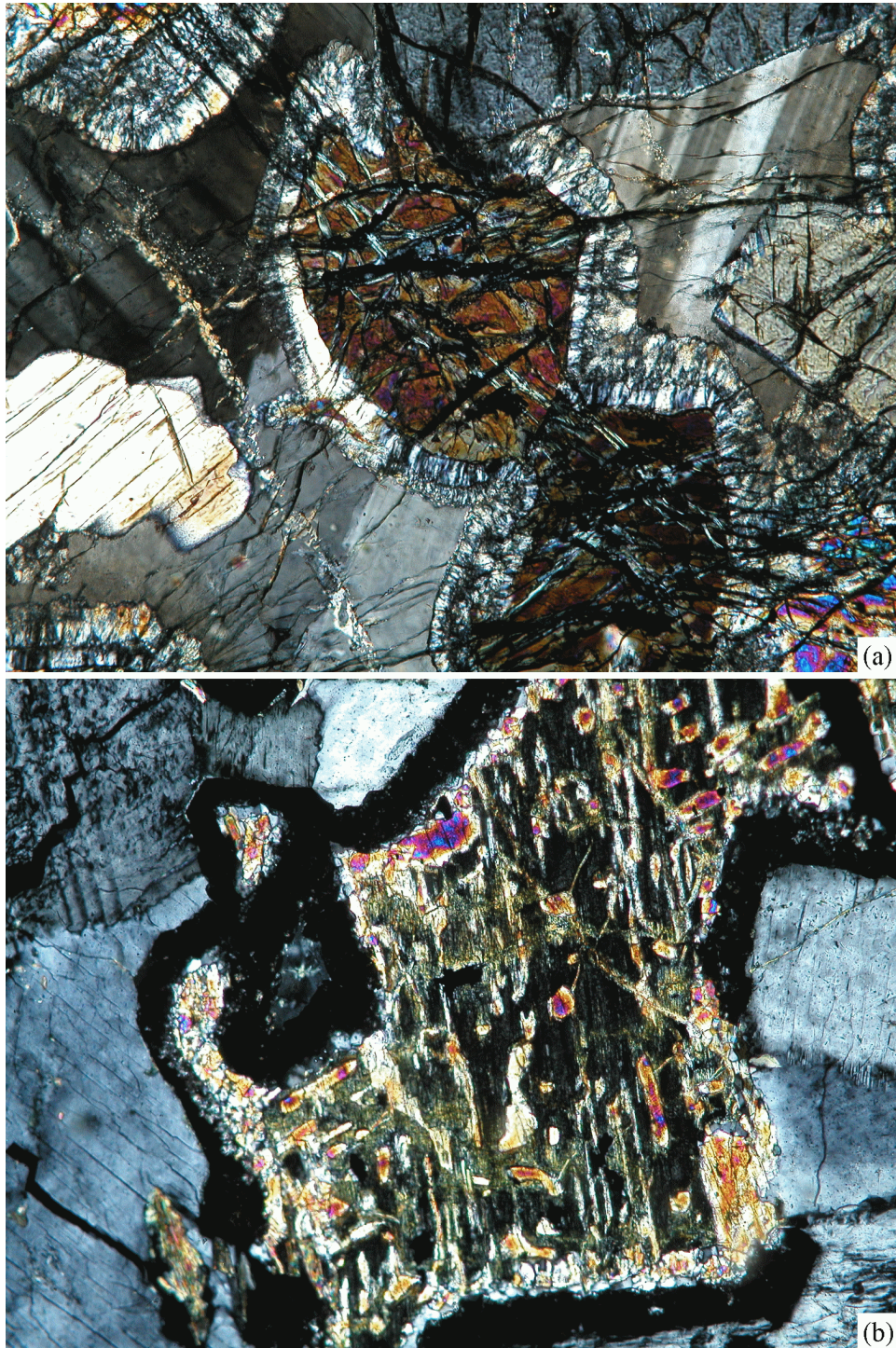
Table 7. Composition (wt%) of rocks from massifs of the drusite complex

Sample	104-1	V-1	V-7	V-8	V-12	V-14	V-16	G-2	L-4	Lod2	Lod3/2	P3	P8	P16	P24-1	P29	P35-9
no.	1	2	3	4	5	6	7	8	9	10	11	12	13	14	15	16	17
Rock	GN	L	L	P	OGN	GN	GN	GN	GN	GN	GN	OGN	L	L	L	PL	OGN
SiO <sub>2</sub>	48.75	49.65	48.85	50.50	46.50	51.65	51.30	53.25	53.80	56.60	52.40	49.10	47.70	48.30	48.65	50.90	51.00
TiO <sub>2</sub>	1.10	0.50	0.68	0.53	0.34	0.39	0.24	0.83	0.80	0.65	0.45	0.50	0.30	0.24	0.24	0.53	0.28
Al <sub>2</sub> O <sub>3</sub>	17.95	8.30	7.40	10.50	17.30	17.65	17.70	7.40	12.70	13.40	19.80	9.35	6.00	5.50	7.00	8.60	10.75
Fe <sub>2</sub> O <sub>3</sub>	0.37	1.20	1.13	0.89	0.13	0.96	1.21	0.75	0.93	1.43	0.44	0.86	4.38	1.78	0.45	1.27	0.89
FeO	10.09	9.68	10.77	9.82	11.04	6.91	6.91	8.73	9.24	6.23	6.53	10.65	8.93	10.26	9.50	9.25	8.42
MnO	0.16	0.18	0.19	0.17	0.14	0.13	0.16	0.18	0.16	0.08	0.10	0.19	0.18	0.20	0.14	0.17	0.13
MgO	7.92	20.00	20.99	16.76	12.13	8.06	9.09	13.19	9.11	6.61	6.84	18.18	25.00	25.65	25.96	20.24	19.09
CaO	10.11	7.91	7.36	8.68	9.23	10.38	9.78	12.49	8.66	7.59	9.45	6.87	5.00	4.89	4.89	6.21	7.25
Na <sub>2</sub> O	1.80	1.13	1.05	1.35	2.19	2.59	2.39	1.97	2.54	3.71	2.71	1.60	0.83	0.73	1.05	1.39	1.56
K <sub>2</sub> O	0.36	0.33	0.34	0.33	0.35	0.20	0.19	0.52	1.28	1.89	0.48	0.65	0.23	0.22	0.29	0.65	0.26
P <sub>2</sub> O <sub>5</sub>	0.12	0.06	0.08	0.08	0.07	0.04	0.03	0.09	0.13	0.13	0.08	0.10	0.06	0.05	0.11	0.10	0.05
Total	98.73	98.94	98.84	99.61	99.42	98.96	99.00	99.40	99.35	98.32	99.28	98.05	98.61	97.82	98.28	99.31	99.68

Sample	P37	P42	P60	P82/7	P82/8	P97	P99	P101	P102	P107	P107/2	P108/7	Pzh13	704	705	708	2-8	742-25
no.	18	19	20	21	22	23	24	25	26	27	28	29	30	31	32	33	34	35
Rock	L	OGN	P	GN	GN	GN	P	L	GN	PL	PL	OGN	MGN	L	OGN	GN	GA	GD
SiO <sub>2</sub>	49.60	52.60	51.66	52.65	53.90	54.00	54.00	49.50	53.80	51.25	50.35	51.00	50.46	49.67	51.42	52.09	48.83	51.89
TiO <sub>2</sub>	0.30	0.24	0.56	0.38	0.83	0.74	0.24	0.20	0.68	0.49	0.47	0.58	2.57	0.31	0.43	0.40	0.12	1.82
Al <sub>2</sub> O <sub>3</sub>	7.30	11.80	7.25	16.60	15.00	16.70	4.70	8.00	16.90	9.30	8.50	10.50	12.84	7.78	11.29	22.07	27.91	13.12
Fe <sub>2</sub> O <sub>3</sub>	1.04	0.10	0.91	1.30	0.78	0.62	0.65	1.85	0.52	0.64	1.28	1.68	1.27	2.65	1.48	1.40	0.00	3.86
FeO	9.95	8.45	8.58	5.22	7.18	6.64	7.96	9.90	6.82	9.77	9.51	9.29	13.40	8.98	7.98	5.13	3.52	11.58
MnO	0.17	0.15	0.19	0.12	0.15	0.13	0.18	0.20	0.13	0.19	0.18	0.17	0.21	0.15	0.14	0.08	0.09	0.15
MgO	22.89	16.92	18.87	8.48	9.19	6.64	26.08	21.91	7.82	19.07	19.93	16.69	4.92	23.76	16.23	4.54	2.08	4.47
CaO	6.67	7.53	9.45	10.60	8.31	9.28	4.01	6.01	8.02	6.01	6.73	6.76	9.34	4.36	7.11	9.14	13.77	8.52
Na <sub>2</sub> O	0.77	1.55	1.02	3.31	2.53	3.08	0.83	1.02	3.13	1.44	1.52	1.90	2.45	0.85	2.11	3.53	1.76	2.91
K <sub>2</sub> O	0.27	0.42	0.47	0.61	1.02	1.12	0.21	0.17	1.07	0.64	0.60	0.78	0.39	0.36	0.47	0.59	0.61	0.79
P <sub>2</sub> O <sub>5</sub>	0.06	0.05	0.07	0.07	0.12	0.12	0.04	0.02	0.11	0.07	0.08	0.09	0.00	0.09	0.13	0.09	0.00	0.12
Total	99.02	99.81	99.03	99.34	99.01	99.07	98.90	98.78	99.00	98.87	99.15	99.44	98.85	98.96	98.79	99.06	98.69	99.35

Note. The sampling sites are in Kandalaksha Bay (1-11, 30-35), Domashnyaya Bay (12-29) of the White Sea; Anisimov Island - 1, Voronii Island - 2-7, Gorelyi Island - 8, Lodeynyi Island - 9-11, Shang Island - 12-14, Yudom-Navolok - 15-29, Pezhostrov Island - 30-34, Cape Tolstik - 35 [Bogdanova, 1996].



**Figure 18.** (a) – Subsolidus coronite texture developing along the contact between olivine and plagioclase. Plagioclase lherzolite from the Shang intrusion, thin section, crossed polarizers. (b) – garnet-hornblende coronite texture around the inverted pigeonite grain. Gabbro-norite, Pezhostrov island, thin section, crossed polarizers.

pletely overlap with the field of boninites from the modern Izu–Bonin island arc, a fact providing evidence of genetic similarities between these rocks.

The spidergrams with trace-element contents normalized

to the primitive mantle (Figure 22) provide additional geochemical criteria pointing to genetic links between the drusite complex and the Burakovsky layered pluton. These links are manifested in the similar character of element distributions

**Table 8.** Trace-element contents (ppm) in rocks from the drusite complex

Sample	V8	V12	V14	V16	AN	G-2	L4	Lod2	Lod3/2	P-3	P-8	P24-1	P-29	P35-9	P-37	P-42	P-97	P-99	P-101	P-107/1	P-108/7
Rock	P	OGN	GN	GN	GN	GN	GN	GN	GN	OGN	L	L	PL	OGN	L	OGN	GN	P	L	PL	OGN
V	217	88	135	110	122	213	208	171	109	204	175	137	160	143	145	159	179	142	133	40	161
Co	69	58	38	53	64	53	45	44	39	78	97	79	62	56	73	66	35	77	84	13	74
Ni	394	341	121	146	694	279	118	74	53	506	867	948	682	486	786	430	94	585	757	14	526
Cu	94	95	49	66	81	67	98	45	33	123	49	77	71	14	36	51	59	39	33	39	33
Zn	92	85	55	75	70	70	77	104	79	108	109	92	78	48	77	82	62	81	95	49	74
Rb	14	20	12	7	16	22	18	42	11	24	10	17	17	15	18	16	10	14	10	228	26
Sr	99	134	213	226	97	178	241	236	257	127	81	71	150	191	106	215	314	54	141	67	179
Y	3	0	1	1	5	7	13	15	1	4	3	5	6	1	0	2	16	3	3	49	4
Zr	45	62	38	0	60	84	110	154	65	58	16	57	77	41	49	32	121	48	28	461	68
Nb	4	1	0	8	3	3	4	9	8	6	5	1	2	3	0	6	3	4	3	15	5
Ba	149	129	87	97	95	215	400	395	173	258	125	147	249	121	114	185	368	123	110	705	293
Pb	2	7	1	5	3	0	7	10	5	2	1	0	2	0	0	5	6	1	3	148	5
Th	1	4	3	1	2	2	7	4	5	5	4	2	8	1	4	3	1	2	2	1	1
Sc	32	19	31	28	20	32	22	26	20	26	21	15	20	23	31	19	25	15	19	0	17

Note. See Table 2 for sampling sites.

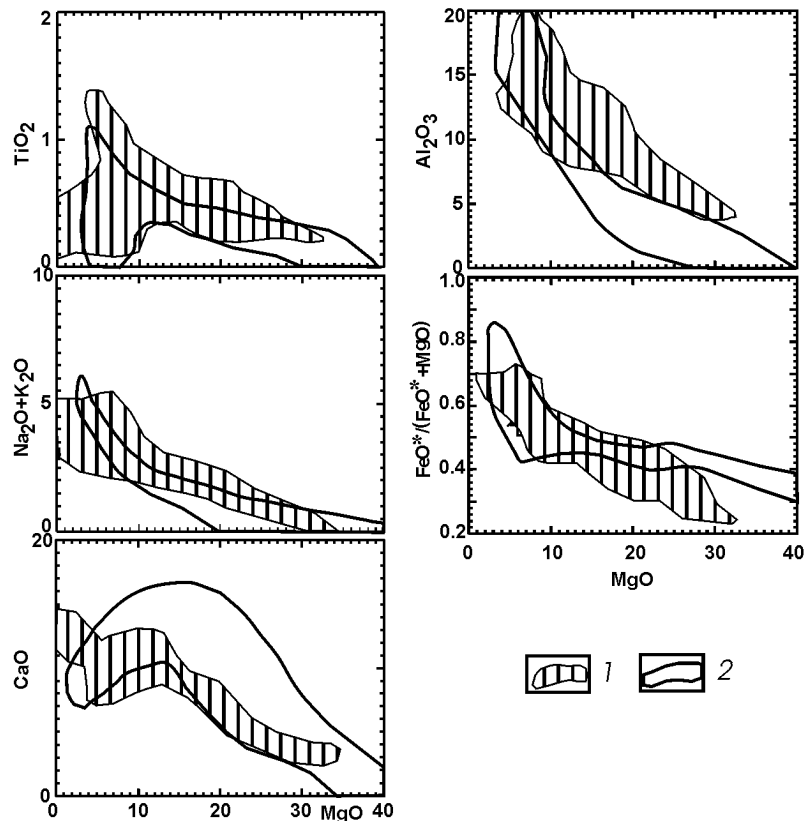


**Figure 19.** Contents of major elements versus MgO in rocks of (1) the drusite complex and (2) the Burakovsky layered intrusion. Here and below, comparative geochemical data on the Burakovsky pluton are given after [Chistyakov *et al.*, 2002].

in the rocks, which are enriched in incompatible elements (Ba, Zr, Th, La, and others) and depleted in HFSE (Nb, Y, and others). The comagmatic character of the rocks of the complex can also be illustrated by their fairly close La/Zr ratios (Figure 23), which are, in turn, closely similar to those in the rocks of the Burakovsky pluton.

Available data indicate that the  $\epsilon\text{Nd}(2.45)$  value for the rocks of the drusite complex ranges from +0.2 to -1.8 [Lobach-Zhuchenko *et al.*, 1998], which is characteristic of the rocks of large layered intrusions in the neighboring cratons [Amelin *et al.*, 1995; Sharkov *et al.*, 1997] and of the coeval basalts in the riftogenic Vetrenyi Belt in the Karelian craton [Puchtel *et al.*, 1997].

Thus, the rock assemblage of the drusite complex in BMB and layered plutons in the nearby cratons show almost unchanging and identical compositional characteristics. These are similar rock assemblages, from ultramafic to leucocratic cumulates and magnetite gabbrodiorites with similar compositions of their minerals. Geochemical data also confirm these similarities: analogously to the rocks of the layered intrusions, the rocks of the drusite complex are low in Ti and Nb and high in LREE at small negative  $\epsilon\text{Nd}(2.45)$  values. All of these features led us to attribute the rocks of the complex to the crystallization products of a silicic high-Mg (boninite-like) series (SHMS).

As was mentioned above (Table 6), the compositions of

the chilled phases of coronite intrusions of the complex generally depend on their type. The gabbronite–anorthosite massifs typically have inner-contact gabbroids with elevated alumina and relatively low magnesia contents, while the lherzolite–gabbronite massifs commonly have low-alumina high-magnesian gabbroids. In other words, the parental melts of the type-I intrusions corresponded to aluminous basalt, compositionally close to the related garnet amphibolites (former volcanic rocks) exposed in Voronii Island (Table 6, analysis 7), and the melts of the type-II bodies were picobasalts. Intrusions with subordinate amounts of ultramafic rocks (in Gorelyi and Lodeinyi islands and in Yudom-Navolok) have intermediate compositions. The chilled zones of the latter two bodies are characterized by elevated  $\text{SiO}_2$  and  $\text{K}_2\text{O}$  contents, which suggest that the melts assimilated the material of the host gneisses. This is consistent with geological and petrographic data on the character of their contacts (see above).

Additional information on the compositions of the melts that produced the complex is provided by metabasite dikes (which likely served as feeders for the younger massifs of the complex) and xenoliths of fine-grained metagabbronites (perhaps, fragments of the material composing these feeders). They are generally close in composition to the chilled zones of most massifs. The exception is the metaperidotite dike in the thinly layered rocks of Anisimov Island

**Table 9.** REE contents (ppm) in rocks from the drusite complex

Sample	V-1	V-7	V-8	V12	V-14	V-16	L-4	Lod3/2	AN	G2	P3	P8	P16	P24-1	P29	P35-9	P37	P42	P97	P99	P101	P108/7
Rock	L	L	P	OGN	GN	GN	GN	GN	GN	GN	OGN	L	L	L	PL	OGN	L	OGN	GN	P	L	OGN
La	3.1	4.1	3.9	3.5	1.8	1.0	11.7	7.2	3.6	10.4	6.7	2.3	2.9	4.9	6.9	3.3	2.8	4.8	14.7	3.3	2.4	9.9
Ce	6.9	9.1	8.6	7.5	3.9	2.0	24.5	15.2	8.0	23.9	14.4	5.4	6.2	9.8	14.7	6.6	6.0	10.0	31.4	6.9	5.4	20.8
Pr	0.90	1.19	1.14	0.94	0.53	0.29	3.00	1.90	1.07	3.25	1.81	0.72	0.81	1.31	1.83	0.86	0.78	1.26	3.94	0.89	0.75	2.55
Nd	3.80	5.10	5.00	4.07	2.50	1.20	11.90	7.53	4.51	13.60	7.40	3.10	3.40	5.28	7.30	3.64	3.20	5.15	15.10	3.65	3.44	10.10
Sm	0.98	1.26	1.17	0.96	0.56	0.32	2.49	1.52	1.15	3.25	1.67	0.71	0.81	1.12	1.49	0.81	0.75	1.04	3.45	0.79	0.88	2.16
Eu	0.31	0.37	0.39	0.42	0.28	0.20	0.63	0.58	0.41	0.88	0.47	0.23	0.25	0.23	0.40	0.22	0.24	0.37	0.98	0.25	0.29	0.62
Gd	1.12	1.37	1.34	1.04	0.70	0.36	2.25	1.40	1.30	2.70	1.71	0.76	0.80	1.03	1.48	0.79	0.80	1.00	3.19	0.75	1.02	2.17
Tb	0.18	0.22	0.22	0.17	0.13	0.07	0.33	0.22	0.21	0.39	0.27	0.12	0.13	0.16	0.22	0.14	0.13	0.15	0.48	0.12	0.16	0.32
Dy	1.16	1.47	1.43	1.15	0.82	0.48	2.08	1.38	1.37	2.25	1.70	0.80	0.86	1.06	1.37	0.81	0.76	0.99	2.91	0.80	0.98	2.08
Ho	0.24	0.32	0.31	0.24	0.18	0.10	0.44	0.28	0.29	0.44	0.36	0.17	0.18	0.21	0.27	0.16	0.17	0.19	0.60	0.16	0.21	0.42
Er	0.73	0.91	0.89	0.72	0.57	0.33	1.23	0.78	0.82	1.17	1.01	0.51	0.52	0.68	0.79	0.47	0.48	0.55	1.59	0.55	0.59	1.18
Tm	0.10	0.13	0.13	0.10	0.09	0.06	0.18	0.11	0.12	0.14	0.15	0.07	0.07	0.09	0.11	0.07	0.06	0.08	0.24	0.08	0.08	0.17
Yb	0.71	0.88	0.85	0.68	0.64	0.37	1.12	0.75	0.78	0.95	1.02	0.51	0.48	0.64	0.74	0.49	0.45	0.45	1.52	0.48	0.59	1.13
Lu	0.11	0.14	0.14	0.09	0.10	0.06	0.17	0.12	0.12	0.13	0.16	0.08	0.07	0.09	0.11	0.06	0.07	0.08	0.23	0.08	0.09	0.17
(La/Nd) <sub>N</sub>	1.56	1.54	1.49	1.65	1.38	1.60	1.88	1.83	1.53	1.46	1.73	1.42	1.63	1.78	1.81	1.74	1.68	1.79	1.86	1.73	1.32	1.87
(Ce/Yb) <sub>N</sub>	2.47	2.63	2.57	2.81	1.55	1.37	5.56	5.15	2.61	6.40	3.59	2.69	3.29	3.89	5.05	3.43	3.39	5.65	5.25	3.63	2.32	4.68

Note. See Table 2 for sampling sites; the ratios are normalized to the chondrite composition [Sun, 1982].

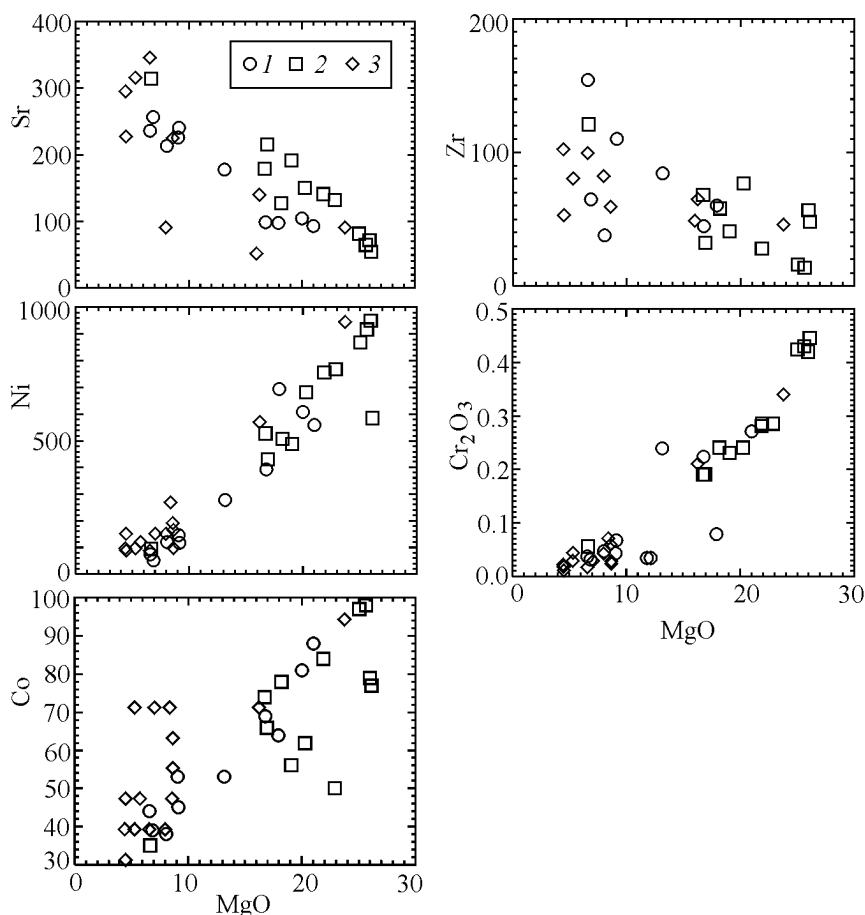


**Figure 20.** Contents of trace elements versus MgO in rocks of the drusite complex. 1 – Drusite bodies in the Kandalaksha Archipelago; 2 – same in the Domashnyaya Bay; 3 – same in the Pezhostrov Island.

(Figure 10), which is the richest in MgO (24.09 wt%, see Table 6, analysis 11). This testifies that some of the melts were picritic and compositionally close to the Early Paleoproterozoic picritic (“komatiitic”) lavas in Karelia [Puchtel *et al.*, 1997]. These melts evidently gave rise to the proper lherzolite bodies of the complex.

## Discussion

### General geological features of the drusite complex.

As was mentioned above, the intrusions of this complex in Belomorje are a component of the large Early Paleoproterozoic Baltic SHMS igneous province. However, manifestations of coeval magmatism of similar character were basically different in the cratons and the mobile belts (BMB and TLMB) between them. While this magmatism produced large layered intrusions, dike swarms, and volcanic sheets in the cratons, in the mobile belts it was characterized, first and foremost, by dispersed magmatic activity, which did not give rise to dike swarms. Volcanic sheets comagmatic with the intrusions of the drusite complex are widespread

along the northeastern boundary of the BMB and its boundaries with the Main Lapland Thrust. These metavolcanics, which were produced by SHMS melts and have ages of 2.45–2.40 Ga, can be traced throughout the whole northeastern shore of Kandalaksha Bay up to Por’ya Bay, where they rest in the bottom of the Kandalaksha Formation. These rocks are known in Finland as the Tana Complex [Barbey and Raith, 1990; Barbey *et al.*, 1984; Belyaev and Kozlov, 1997; Sharkov and Smolkin, 1997]. Intense Svecofennian metamorphism transformed them mostly into garnet amphibolites, which locally exhibit relict volcanic textures [Priyatkina and Sharkov, 1979]. Tectonic blocks of these amphibolites also occur among migmatites in some islands of the Kandalaksha Archipelago, for example, in Voronii Island (authors’ data). All of these facts suggest that intrusions of the drusite complex were formed simultaneously with lava flows on the surface.

**Conditions under which the drusite complex was produced.** Unlike other magmatic complexes of the BLIP, some features of the drusite complex characterize its rocks as the crystallization products in a mobile environment. These features are as follows: (1) small sizes of the bodies and their wide lateral distribution; (2) the petrography of the

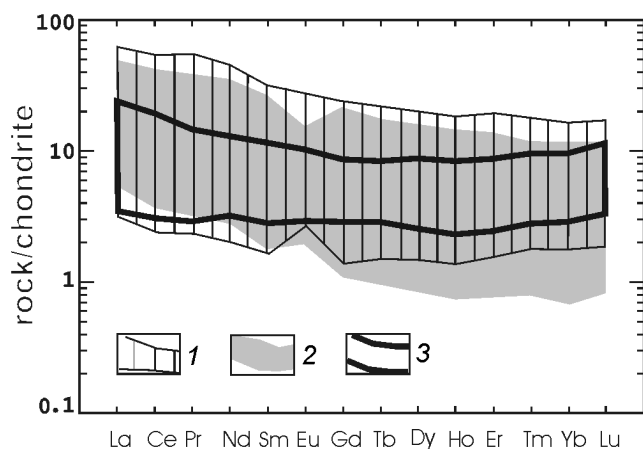


**Figure 21.** Chondrite-normalized REE patterns for rocks of the drusite complex. 1 – Drusite complex; 2 – Burakovsky pluton; 3 – boninites from the Izu-Bonin island arc [Murton *et al.*, 1992].

rocks suggests their rapid solidification; (3) the morphology of the bodies often implies that these bodies filled detachment voids in folds; (4) numerous distortions of their primary magmatic layering; (5) the bodies themselves and their host rocks are often cut by basite dikes along shear zones, with these dikes also produced by the SHMS melts; (6) the mafic-ultramafic bodies of the complex had different original orientation and were variably reworked, which suggests that there are a number of intrusion generations of different ages (in this situation, the aforementioned dikes could have served as feeders for younger intrusions); and (7) the spatial distribution of the intrusions is controlled by different Early Paleoproterozoic stress field orientations in the BMB.

**The character of the contacts of intrusions in the drusite complex.** The host rocks of these intru-

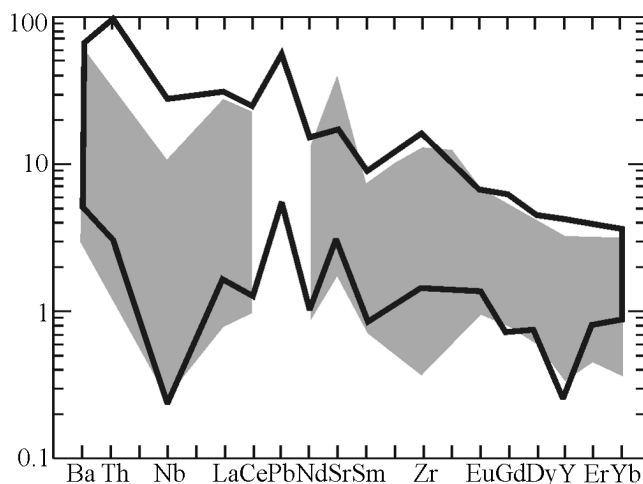


**Figure 22.** Spidergram of primitive mantle-normalized contents of trace elements in rocks of the drusite complex and the Burakovsky pluton (dark).

sions are most often Archean tonalitic granite-gneisses and migmatites (gray gneisses). More rarely, these intrusions cut aluminous garnet-biotite gneisses, whose protoliths were supracrustal rocks. This is consistent with the occurrence of metasedimentary xenoliths in the anorthosites exposed in Medyanka Island (see above).

Although the primary intrusive contacts of the bodies with their host rocks are preserved only rarely, such contacts were detected, nevertheless, at intrusions of all types. The host rocks themselves could be quite cold during the emplacement of the drusite complex, and this caused the development of chilled zones and apophyses (Gorelyi Island). In other instances, they could be moderately heated, as follows from manifestations of anatexis and the development of diverse hybrid rocks (Yudom-Navolok Massif), or even hot, which could result in diffusive contacts between the mafic intrusions and the host plagiogneisses (the “hot contact” in Lodeinyi Island). These observations furnish geological evidence that the magmatic process was fairly protracted. It is also pertinent to mention that both the rocks of the complex itself and the host Archean rocks most often show evidence of Svecofennian metamorphism [Korikovskiy, 2004].

The tectonic contacts of the drusite bodies are marked with the shearing of both the host rocks and the rocks of the complex and with the amphibolization of these rocks. As was demonstrated above, these contacts are often associated with zones of Karelian migmatization, often with breccias, in which angular fragments of drusite bodies are transformed into amphibolites and cemented by granitic material. In contrast to the ancient plagiomigmatites, this material usually consists of pink potassic granitoids. More or less fresh magmatic rocks with primary magmatic textures and structures are usually preserved only in the central portions of the bodies, which sometimes retain the primary magmatic layering. When the primary contacts are also preserved, it can be seen that the layering is oriented conformably with these contacts.

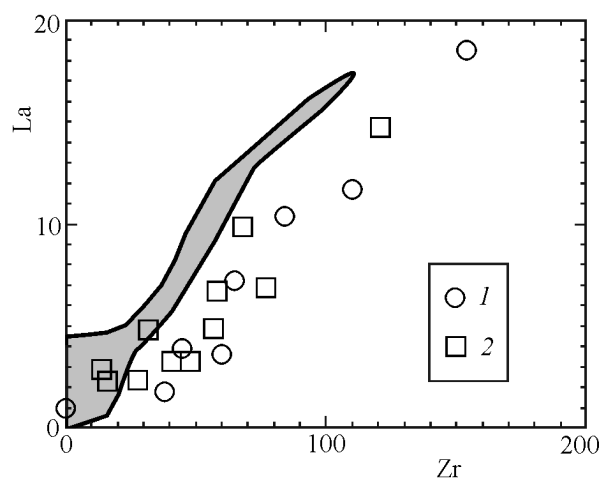


**Figure 23.** La versus Zr for rocks of the drusite complex. 1 – Kandalaksha Archipelago; 2 – Domashnyaya Bay. The contoured field corresponds to the Burakovsky layered intrusion.

**The age of the drusite complex.** The age of the magmatic crystallization of the intrusive bodies varies from 2.45 to 2.36 Ga. The Pezhostrov gabbro-norite–anorthosites crystallized at  $2452 \pm 20$  Ma (U–Pb zircon dates [Alexejev *et al.*, 2000]). The age of the Voronii Island rocks is approximately  $2460 \pm 10$  Ma (see above); the Tupaya Bay plagioclase lherzolites were dated at  $\sim 2451 \pm 17$  Ma [Bibikova *et al.*, 1993]; the Kovdozero lherzolite–gabbro-norite massif has an age of  $2440 \pm 10$  Ma [Kaulina and Kudryashova, 2000]; the Shobozero gabbro-norite massif was dated at  $2435 \pm 5$  Ma [Slabunov *et al.*, 2001]; the gabbro-norite massif in Lodeinyi Island has an age of  $2442 \pm 3.6$  Ma (see above); the gabbro-norites in Kochinnyi Cape in the northeastern shore of Kandalaksha Bay was dated at  $2433 \pm 4$  Ma [Kaulina, 1996]; the magnetite gabbrodiorites exposed at Cape Tolstik have an age of  $2434 \pm 7$  Ma [Bibikova *et al.*, 1993]; the age of the Krivoi Island intrusion in Por'ya Bay is  $2365 \pm 25$  Ma [Kaulina and Bogdanova, 1999]; and the youngest age of  $2356 \pm 4$  Ma was yielded by the gabbro-norite intrusion of the Zhemchuzhnyi Massif in the Kola Peninsula [Balaganskii *et al.*, 1997]. All of these age values coincide with the ages of large layered intrusions in the nearby Kola craton [Amelin *et al.*, 1995; Chistyakov *et al.*, 2000]. The bodies of the main generation are often intersected by pink potassic granites with an age about 2.41 Ga [Bibikova *et al.*, 1993; Zinger *et al.*, 1996].

As follows from the facts presented above, SHMS magmatism in the BMB and the neighboring Karelian craton spanned a significant age interval in the Early Paleoproterozoic, starting from at least 2.46 Ga (Pezhostrov Massif) to 2.36 Ga (Zhemchuzhnyi Massif in the Kola Peninsula), i.e., approximately 100 m.y. As is evident from the above materials, there seems to be no correlations between the ages of the intrusions and their compositions.

The feeders of the new intrusions are partly preserved in the form of dikes cutting across already-solid intrusions of the drusite complex, which were still not deformed (as in Anisimov Island) or were sheared (blastomylonitized), with these zones intruded by the dikes, as can be clearly seen in the Pezhostrov Island and Cape Tolstik intrusions. Fragments of analogous dikes were also found in the host rocks in the form of amphibolite boudins. The magmatic activity seems to have continued and was not been interrupted by the reorientation of the stress field in the upper crust. This ensured the wide spread of bodies of the drusite complex within the BMB. Indirect evidence of the long-lasting character of drusite magmatism is served by the observed differences in the intrusive contacts of the bodies, a fact also documented by other researchers.

The primary layering of the intrusions is oriented along the following four major directions: roughly westward (Anisimov Island, Domashnyaya Bay, Kovdozero, and others), roughly northward (Pezhostrov and Lodeinyi islands), northwestward (Voronii Island and Ovechii Island massifs, Cape Tolstik Massif, and others), and northeastward (Gorelyi Island, gabronorite body in Lodeinyi Island, and others). In this context, it is pertinent to mention that exactly these major directions were typical of the Early Paleoproterozoic deformations during the main evolutionary stages of the BMB [Volodichev, 1990]. As was mentioned

above, the spatial distribution of drusite bodies also corresponds to these directions. This led us to conclude that there is a good correlation of the orientation and spatial distribution of the intrusions with the orientation of the main stress fields in the Early Paleoproterozoic in the BMB.

The main episode of the metamorphic reworked of the BMB took place at about 1.9–1.8 Ga ago [Alexejev *et al.*, 1999; Bibikova *et al.*, 2004; Bogdanova, 1996; Kaulina and Kudryashov, 2000; Korikovskiy, 2004; Larikova, 2000; Zinger *et al.*, 1996] and was related to the development of the Svecofennian (Late Paleoproterozoic) Main Lapland Thrust. The corona textures and amphibolization of the mafic rocks seem to have developed during exactly this time. This is consistent with the age values obtained for metamorphic apatite, garnet, and rutile in the anorthosites exposed in the Pezhostrov and Voronii islands (see above). Also, it was likely then that most basite bodies in the Kandalaksha part closest to the fault were boudinaged and acquired a secondary northwestern orientation, conformable with the trend of the fault. The intrusive rocks underwent amphibolization and migmatization along the detachment faults, as is seen, for example, in the Gorelyi Island intrusion. This example clearly demonstrates that the intrusion was still hot during its synmetamorphic deformations, and, thus, the primary magmatic layering became bent along the detachment fault surface. Away from the fault, for example, in Domashnyaya Bay, overprinted processes were weaker.

**Distinctive structural features of the BMB magmatic systems.** The obvious similarities between the rocks of the drusite complex and layered intrusions in the cratons suggest that all of these rocks were produced by similar SHMS melts. According to geochemical and isotopic–geochemical data, these melts were generated by the large-scale assimilation of Archean crustal rocks by ultramafic mantle melts [Amelin and Semenov, 1996; Puchtel *et al.*, 1997; Sharkov *et al.*, 1997]. This, in turn, implies that the magma-generating systems beneath the cratons and BMB should also have been similar.

The most probable mechanism of the origin of these melts was the ascent of magma chambers through the crust according to the zone-refinement mechanism [Sharkov *et al.*, 1997], i.e., by means of the simultaneous melting of the roof rocks and crystallization of the melt near the bottom (Figure 24). This ascent (“floating”) should, perhaps, have stopped as soon as the chambers attained the predominantly sialic crust, because the upper parts of these chambers started to produce thick layers of light granitic melts that could not any more be involved in the overall convection and, thus, stopped the zone-refinement mechanism [Sharkov, 2003]. This idea finds further support in the fact that the evolution of both large layered complexes in the cratons and many bodies in the drusite complex (for example, the Cape Tolstik intrusion, see above) ended with potassic granites. The potassic character of these granites was, perhaps, caused by the experimentally proved operation of K and Na counterdiffusion across the interface between the basaltic and granitic melts [Bindeman and Davis, 1999].

The differences in the character of intrusive magmatism were obviously related to the mobility of the environments

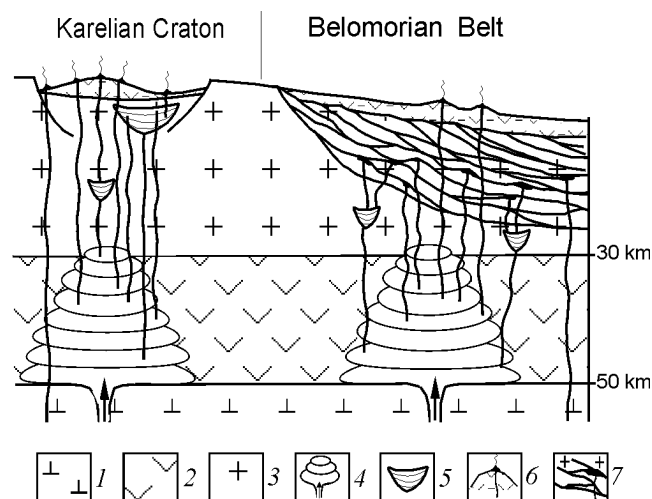


**Figure 24.** Model for the structure of magmatic systems beneath cratons and intercratonic mobile belts of the Baltic Shield (after [Sharkov, 2003]). 1 – Ancient lithospheric mantle; 2 – Archean basite lower crust; 3 – Archean sialic crust; 4 – region where the magma chambers ascend according to the floating-zone mechanism; 5 – layered intrusions; 6 – sedimentary–volcanic rocks and lava plateaus; 7 – zone of tectonic flowage of the Belomorian belt with drusite bodies (black).

through which the melts passed en route from the magma-generating regions to the surface. In rigid cratons, the melts ascending from evolving deep-seated chambers accumulated in the same intrusive chambers, which served as structural traps and progressively increased in size with the arrival of new magma portions. This process resulted in the origin of large intrusive bodies, which included the crystallization products of all of these melts and the whole set of corresponding cumulates. In places, the complexes were formed by two or more large intrusions, as the Burakovsky and Monchegorsky complexes [Chistyakov *et al.*, 2002; Sharkov *et al.*, 2002]. Judging by isotopic–geochemical data, they were long-lived magmatic centers, whose lifetime was ~50 m.y.

The same rocks occur in the BMB as small individual intrusions. Evidently, as the material of the belt remained mobile for a long time, melt portions coming from beneath could be accommodated only in small chambers, which were controlled by local heterogeneities (folds, detachments, local extension zones, etc.) generated in the process of the tectonic flowage of the country rocks. Furthermore, these chambers were constantly displaced, and this also precluded the focused accumulation of significant melt volumes and the origin of large magmatic bodies. Nevertheless, judging from the occurrence of intrusions with layered structures, crystallizing differentiation in these bodies still has enough time to proceed. In the mobile environment, part of the still-

liquid melt could be forced into other chambers and produce individual bodies, in which differentiation processes could continue. Consequently, numerous compositionally different small rootless intrusions that were formed at different depths within this belt were prone to be localized along the directions of the main stress field orientation during certain evolutionary episodes of the BMB.

This leads to the unexpected conclusion that all Early Paleoproterozoic tectonic processes in the BMB were restricted exclusively to its upper level and did not affect magmatic systems in the basement. In other words, the processes of gently inclined tectonic flowage of the crustal rocks occurred only in the upper crust, which was underlain by a stable lithospheric region, in which SHMS magmas were produced and underwent differentiation. This is in good agreement with geophysical data indicating that intense nappe–fold deformations acted there only within the uppermost 20–25 km interval, which was underlain by a geophysically homogeneous basement [Berzin *et al.*, 2001].

Judging from the occurrence of subsolidus spinel–pyroxene corona textures in the rocks of the drusite complex, the intrusions crystallized under a pressure of 6–7 kbar, which corresponds to the lithostatic pressure at depths of 21–24 km [Sharkov *et al.*, 1994]. These depths were, perhaps, even shallower, because the pressure value in the highly mobile material of the Belomorian Belt was determined not only by the load of the overlying rocks but also by the stress. The depths of the chambers from which the magmas came could hardly be greater than 50 km, because, according to experimental data on such melts, their residue under high pressures should contain garnet [Green and Ringwood, 1967], which is in conflict with the REE patterns for rocks of the drusite complex. This implies that the tectonic flowage zone during the origin of the drusite complex was most probably no thicker than 35–40 km. A generalized model of Early Paleoproterozoic magmatic systems in the Baltic Shield beneath cratons and transitional intercratonic mobile belts, for example, BMB, is presented in Figure 24.

Recently obtained data on the coronite gabbroid dikes in the BMB indicate that some of them (also often assigned to the drusite complex) have an age of 2.1 Ga [Stepanova *et al.*, 2003]. The composition of these rocks is, however, principally different from the composition of the “classic” Belomorian drusites, and they were produced by high-Fe and high-Ti tholeiitic magmas, analogous to the basalts occurring in Jatulian volcanic complexes in the Karelian and Kola cratons. This suggests that the character of the mantle sources beneath the BMB and neighboring cratons had then significantly changed, and another large magmatic province was formed in the Baltic Shield in relation to the ascent of a newly formed superplume.

The dikes of ferrous gabbroids were obviously emplaced shortly before the fundamental change in the style of the magmatic activity in the Baltic Shield at 2.0–1.9 Ga. After this, a large compression zone was formed (the Lapland Fault) and new metamorphic zoning developed, which involved both the bodies of the drusite complex itself and these younger dikes.

## Conclusions

1. The Belomorian drusite complex (2.45–2.35 Ga) comprises numerous small synkinematic mafic and ultramafic intrusions widespread throughout the BMB area. Their volcanic analogues seem to be metavolcanic rocks (garnet amphibolites) of the Kandalaksha formation and the Tana Complex in Finland, which are exposed along the northern BMB margin.

2. The intrusions can be subdivided into two major types. Type I comprises plagioclase lherzolites (Ol±Crt, Ol+Opx±Crt, and Ol+Opx+Cpx±Crt cumulates), pyroxenites, melanocratic gabbronorites (Opx±Cpx cumulates), olivine gabbronorites (Ol+Opx+Pl±Cpx cumulates), and gabbronorites (Opx+Pl±Cpx cumulates). Type II includes volumetrically predominant norites, gabbronorites anorthosites, and gabbronorite–anorthosites (Pl cumulates) and subordinate amounts of magnetite gabbrodiorites (Opx+Pl+Cpx+Mag cumulates).

3. The composition and quantitative proportions of the rocks making up the drusite complex roughly correspond to those in large layered intrusions in the neighboring cratons. Both rock groups are similar in petrography, geochemistry, and isotopic geochemistry, which suggests that all of these rocks were produced by the same type of parental magmas: silicic high-Mg (boninite-like) series (SHMS). However, the rocks of the drusite complex display a clearly pronounced tendency toward forming individual bodies with the corresponding compositions of the inner-contact rocks. This complex was emplaced and then crystallized in a mobile environment, which caused the small sizes of the bodies and their wide distribution within the belt.

4. Intrusive contacts of the bodies are preserved rarely but were found, nevertheless, at intrusions of all types. Depending on the temperature of the host Archean rocks, the contact relations could be of the following three types: (i) at the emplacement time, the host rocks were quite cold and, thus, ensured the development of chilled zones and apophyses (as at the body in Gorelyi Island); (ii) the host rocks were heated to temperatures high enough for anatexis of the wall-rock gneisses to occur and a diversity of hybrid rocks to be formed (Yudom-Navolok Massif); and (iii) the host rocks were hot and likely induced counterdiffusion of components between the mafic intrusions and the host plagiogneisses (the “hot contact” in Lodeinyi Island).

5. Upon their solidification, the intrusions of the complex and their host gneisses and migmatites were involved in tectonic flowage processes under amphibolite-facies conditions at elevated pressures. As a result, most of the bodies have tectonized contacts, and their rocks were blastomylonitized and amphibolized. Relatively little altered rocks are preserved only in the central portions of the bodies and are characterized by widespread coronite (drusite) textures along the grain boundaries of primary magmatic minerals.

6. The complex was produced not instantaneously but over a time span of approximately 100 m.y. There seems to be no correlations between the composition of the melts and the time of their emplacement. The spatial distribution of the bodies exhibits a clearly pronounced tendency toward

their arrangement parallel to the directions along which the main stress fields were oriented during the major deformational episodes of the BMB in the Early Paleoproterozoic.

7. The rocks of the drusite complex are a component of the large Baltic igneous SHMS province, which suggests that the magma generating zones beneath the cratons and BMB were similar. Within the mobile environment of the BMB, melt portions coming from beneath were accommodated in small chambers, whose setting was controlled by local structural heterogeneities (detachment faults, cavities in folds, local extension zones, etc.), which were produced by the tectonic flowage of the host rocks. These chambers were constantly displaced and, thus, could not accumulate enough melt to produce large intrusive bodies.

8. The origin of the Baltic SHMS province is thought to have been related to a mantle superplume of strongly depleted ultramafic material beneath the eastern part of the shield. The extension of the rigid cratonic crust above the laterally spreading head of the plume gave rise to graben-shaped volcano-sedimentary structures, dike swarms, and large layered intrusions. Areas adjacent to the zones of downgoing mantle flows were marked by the development of mobile belts (BMB and TLMB) with a dispersed type of magmatism.

**Acknowledgments.** The authors thank the Direction and the staff of the Kandalaksha Nature Reserve, especially A.S. Koryakin, and V. Ya. Berger, the head of the Kartesh Biological Observatory of the Zoological Institute, Russian Academy of Sciences, for help during the fieldwork. The authors also thank S. P. Korikovskiy, Corresponding Member of the Russian Academy of Sciences, and Dr. O. A. Lukanin, who reviewed the manuscript and expressed valuable remarks. This research was financially supported by the Russian Foundation for Basic Research (project nos. 01-05-64673 and 04-05-64581), the Federal Program for Support of Scientific Schools (Grant 1251.2003), and Program 5 of the Division for Earth Sciences of the Russian Academy of Sciences.

## References

- Alexeev, N. L., S. B. Lobach-Zhuchenko, E. S. Bogomolov, N. A. Arestova, G. M. Drugova, Yu. V. Amelin, and V. F. Guseva (1999), Phase and isotopic (Nd) equilibria in drusites from the Tolstik Massif and the Tupaya Bay area, NW Belomorie, Baltic Shield, *Petrology*, 7, 3–23.
- Alexeev, N. L., T. F. Zinger, B. V. Belyatsky, and V. V. Balaganskii (2000), Age of crystallization and metamorphism of the Pezhostrov gabbro-anorthosites, northern Karelia, Russia, in SVEKALAPKO 5th meeting, *Abstracts*, p. 3, Lammi.
- Amelin, Yu. V., L. M. Heaman, and V. S. Semenov (1995), U–Pb geochronology of layered intrusions in the eastern Baltic Shield: implications for the timing and duration of Paleoproterozoic continental rifting, *Precambrian Res.*, 75, 31–46.
- Amelin, Yu. V., and V. S. Semenov (1996), Nd and Sr isotope geochemistry of mafic layered intrusions in the eastern Baltic Shield: implications for the sources and contamination of Paleoproterozoic mafic magmas, *Contrib. Mineral. Petrol.*, 124, 255–272.
- Balaganskii, V. V., N. M. Kudryashov, Yu. V. Balashov, et al. (1997), On the age of the Zhemchuzhnyi drusite massif, NW

- Belomorie: U–Pb isotopic data and geological implements, *Geochem. Int.*, *35*, 158–168.
- Barbey, P., J. Convert, B. Moreau, et al. (1984), Petrogenesis and evolution of an Early Proterozoic collisional orogen: the Granulite Belt of Lapland and the Belomorides (Fennoscandia), *Bull. Geol. Soc. Finland*, *56*, 161–188.
- Barbey, P., and M. Raith (1990), The Granulite Belt of Lapland, in *Granulites and Crustal Evolution*, edited by D. Veilzent and Ph. Vidal, pp. 111–132, Kluwer, Dordrecht.
- Bayanova, T. B., V. I. Pozhilenko, V. F. Smolkin, et al. (2002), *Geology of Mining Districts in Murmansk Oblast', Appendix 3, Catalogue of Geochronologic Data on the NE Baltic Shield* (in Russian), edited by F. P. Mitrofanov, 53 pp., Apatity.
- Belyaev, O. A., and N. E. Kozlov, (1997), Geology, geochemistry and metamorphism of the Lapland Granulite Belt and adjacent areas in the Vuosto area, northern Finland, *Geol. Surv. Finland*, *138*, 24 p.
- Berzin, R. G., A. K. Suleimanov, N. G. Zamozhnyaya, et al. (2001), Geophysical studies along the 4B SVEKALAPKO regional profile, in *Deep Structure and Crustal Evolution of the Eastern Part of the Svecofennian Shield: Kem'-Kalevala Profile* (in Russian), pp. 39–63, Karelian Division of the Russ. Acad. Sci., Petrozavodsk.
- Bibikova, E. V., S. V. Bogdanova, V. A. Glebovistikii, S. Claesson, and T. Skiold (2004), Evolutionary stages of the Belomorian Mobile Belt, Baltic Shield: U–Pb isotopic dating of zircon on a NORDSIM ion probe, *Petrology*, *12*, in press.
- Bibikova, E. V., S. Claesson, V. A. Glebovistikii, et al. (2001), Isotopic dating of the Svecofennian stage in the transformations of the Belomorian Belt at the Baltic Shield, *Geochem. Int.*, *39*, 1116–1119.
- Bibikova, E. V., T. Skiold, S. V. Bogdanova, et al. (1993), Geochronology of the Belomorides: an interpretation of the multistage geological history, *Geochem. Int.*, (10), 1393–1412.
- Bindeman, I. N., and A. M. Davis (1999), Convection and redistribution of alkalis and trace elements during the mixing of basaltic and granitic melts, *Petrology*, *7*, 99–110.
- Bogatikov, O. A., V. I. Kovalenko, E. V. Sharkov, and V. V. Yarmolyuk (2000), *Magmatism and Geodynamics, Terrestrial Magmatism Throughout the Earth's History*, 511 pp., Gordon and Breach, Amsterdam.
- Bogdanova, S. V. (1996), High-grade metamorphism of 2.45–2.4 Ga age in mafic intrusions of the Belomorian Belt in the northern Baltic Shield, in *Precambrian Crustal Evolution in the North Atlantic Region, Geol. Soc. Spec. Publ.*, no. 112, edited by T. S. Brewer, pp. 69–90.
- Bogina, M. M., I. S. Krasvskaya, E. V. Sharkov, et al. (2000), Vein granites of the Burakovsky layered massif, southern Karelia, *Petrology*, *4*, 366–383.
- Chistyakov, A. V., O. A. Bogatikov, T. L. Grokhovskaya, et al. (2000), Burakovsky layered pluton in S Karelia as a result of spatial combination of two bodies: petrological and isotopic–geochemical data, *Dokl. Russ. Akad. Nauk.*, *372*, 698–704.
- Chistyakov, A. V., E. V. Sharkov, T. L. Grokhovskaya, et al. (2002), Petrology of the Europe-largest Burakovka Early Paleoproterozoic layered pluton (southern Karelia, Russia), *Russian J. Earth Sci.*, *1*, URL: <http://rjes.wdcb.ru/>
- Efimov, M. M., M. N. Bogdanova, and S. V. Bogdanova (1987), Periodicity and types of Archean magmatism in NW Belomorie (Tolstik testing ground), in *Basite-Hyperbasite Magmatism in the Major Tectono-Stratigraphic Zones of the Kola Peninsula* (in Russian), pp. 13–29, Kola Research Center., Acad. Sci. USSR, Apatity.
- Green, D. H., and W. H. Hibberson (1970), The instability of plagioclase in peridotite at high pressure, *Lithos*, *5*, 209–222.
- Green, D. H., and A. E. Ringwood (1967), Genesis of basaltic magmas, *Contrib. Mineral. Petrol.*, *15*, 103–190.
- Kaulina, T. B. (1996), Dating results on rocks from Cape Tolstik, NW Belomorie, in *Problems of the Geology in the Karelia-Kola Area* (in Russian), edited by A. I. Golubev, pp. 64–71, Kola Research Center, Russ. Acad. Sci., Petrozavodsk.
- Kaulina, T. B., and M. N. Bogdanova (1999), Newly obtained U–Pb isotopic data on magmatic and metamorphic processes in NW Belomorie, *Dokl. Russ. Akad. Nauk.*, *366*, 677–679.
- Kaulina, T. B., and N. M. Kudryashov (2000), Evolutionary history of the Belomorian Complex, paper presented at the III all-Russia conference “General problem in the stratigraphic subdivision of the Precambrian”, pp. 100–102, Apatity, (in Russian).
- Korikovskiy, S. P. (2004), Prograde equilibria in garnet–clinopyroxene–plagioclase amphibolites of the Belomorian Complex, NW Belomorie, islands in Kandalaksha Bay: P–T parameters and metamorphic stages, *Petrology*, *12*, in press.
- Larikova, T. L. (2000), Genesis of drusite (coronite) textures around olivine and orthopyroxene during metamorphism of gabbroids in northern Belomorie, Karelia, *Petrology*, *4*, 430–448.
- Lobach-Zhuchenko, S. B., N. A. Arestova, V. P. Chekulaev, et al. (1998), geochemistry and petrology of 2.40–2.45 Ga magmatic rocks in the north-western Belomorian Belt, Fennoscandian Shield, Russia, *Precambrian Res.*, *92*, 223–250.
- Malov, N. D., and E. V. Sharkov (1978), The composition of parental melts and crystallization conditions of Early Precambrian intrusions of the drusite complex in Belomorie, *Geokhimiya* (in Russian), (7), 1032–1039.
- Mitrofanov, F. P., and V. I. Pozhilenko (Eds.) (1991), *The Voche-Lambina Archean Geodynamic Testing Ground in the Kola Peninsula* (in Russian), 196 pp., Kola Research Center., Acad. Sci. USSR, Apatity.
- Murton, B. J., D. W. Peete, R. J. Arculus, et al. (1992), Trace-element geochemistry of volcanic rocks from Site 786: the Izu-Bonin forearc, in *Proc. ODP, Sci. Results*, vol. 125, edited by P. Fryer, J. A. Pearce, L. A. Stokking, et al., pp. 211–236, College Station, TX (Ocean Drilling Program).
- Priyatkina, L. A., and E. V. Sharkov (1979), *Geology of the Lapland Deep Fault at the Baltic Shield* (in Russian), 127 pp., Nauka, Leningrad.
- Puchtel, I. S., K. M. Haase, A. W. Hofmann, et al. (1997), Petrology and geochemistry of crustally contaminated komatiitic basalts from the Vetrenyi Belt, southeastern Baltic Shield: evidence for an Early Proterozoic mantle plume beneath the rifted Archean continental lithosphere, *Geochim. Cosmochim. Acta*, *61*, 1205–1222.
- Sal'e, M. E., D. P. Vinogradov, and M. N. Gavrilina (1983), *Fractionation of Oxygen Isotopes in Minerals from Polymetamorphic Complexes* (in Russian), 135 pp., Nauka, Leningrad.
- Sharkov, E. V. (1980), *Petrology of Layered Intrusions* (in Russian), 183 pp., Nauka, Leningrad.
- Sharkov, E. V. (2002), The role of surface formation energy in magmatic processes, I. Melt solidification, *Izv. Vyssh. Uchebn. Zaved. Geol. Razvedka* (in Russian), (2), 70–82.
- Sharkov, E. V. (2003), Layered intrusions as transitional magma chambers above the local plumes of a large igneous rock province: evidence from the Early Paleoproterozoic province of silicic highly magnesian rock series in the Baltic Shield, *Russian J. Earth Sci.*, *5*, 1–10.
- Sharkov, E. V., O. A. Bogatikov, and I. S. Krassivskaya (2000), The role of mantle plumes in Early Precambrian Tectonics in the Baltic Shield, *Geotectonics*, *34*, 85–105.
- Sharkov, E. V., V. V. Lyakhovich, and G. V. Ledneva (1994), Petrology of the Early Proterozoic Belomorian drusite complex: a case study of the Pezhostrov Massif, N Karelia, *Petrology*, *2*, 454–475.
- Sharkov, E. V., and V. F. Smolkin V.F. (1997), The Early Proterozoic Pechenga-Varzuga belt: a case of Precambrian back-arc spreading, *Precambrian Res.*, *82*, 133–151.
- Sharkov, E. V., V. F. Smolkin, and I. S. Krassivskaya (1997), Early Proterozoic province of high-Mg boninite-like rocks in the eastern part of the Baltic Shield, *Petrology*, *5*, 448–465.
- Sharkov, E. V., V. F. Smolkin, A. V. Chistyakov, et al. (2002), Geology and metallogeny of the Monchegorsk layered complex, in *Russian Arctic: Geological History, Mineralogy, and Geoecology* (in Russian), pp. 485–494, VNIIOkeanologiya, St.-Petersburg.
- Sharkov, E. V., G. A. Snyder, L. A. Taylor, and T. F. Zinger (1999), An Early Proterozoic large igneous province in the eastern Baltic Shield: Evidence from the mafic drusite complex, Belomorian Mobile Belt, Russia, *Int. Geol. Rev.*, *41*, 73–93.

- Shurkin, K. A., V. L. Duk, and F. P. Mitrofanov (1960), Materials to the geology and petrography of Archean gabbro–labradorites in N Karelia, *Tr. Lab. Geol. Dokembriya* (in Russian), issue 9, pp. 120–149, Akad. Nauk SSSR.
- Shurkin, K. A., N. V. Gorlov, M. E. Sal'e, et al. (1962), *Belomorian Complex in N Karelia and the SW Kola Peninsula: Geology and Pegmatite Reserves* (in Russian), Akad. Nauk SSSR, 306 pp., Moscow–Leningrad.
- Shurkin, K. A., and R. Z. Levkovskii (1966), On the age of gabbro–labradorite intrusions in Belomorie, in *Geological Problems and the Distribution of Mineral Reserves in Karelia* (in Russian), pp. 267–289, Kareliya, Petrozavodsk.
- Slabunov, A. I., A. N. Larionov, E. V. Bibikova, et al. (2001), Geology and geochronology of the Shobozero lherzolite–gabbro–labradorite massif in the Belomorian Mobile Belt, in *Geology and Mineral Resources of Karelia*, vol. 3, edited by A. I. Golubev and V. V. Shchiptsov, pp. 3–14, Karelian Research Center, Russ. Acad. Sci.
- Smolkin, V. F., Zh. A. Fedotov, Yu. N. Neradovsky, et al. (2004), *Layered intrusions of the Monchegorsk ore region* (in Russian), Pt. 1 and 2, pp. 177–178, Kola Science Center RAS, Apatity.
- Stepanov, V. S. (1981), *Precambrian Mafic Magmatism in W Belomorie* (in Russian), 216 pp., Nauka, Leningrad.
- Stepanova, A. V., A. N. Larionov, E. V. Bibikova, et al. (2003), Early Proterozoic (2.1 Ga) Fe–tholeiite magmatism in the Belomorian province of the Baltic Shield: geochemistry and geochronology, *Dokl. Russ. Akad. Nauk*, 390, 528–532.
- Sun, S. S. (1982), Chemical composition and origin of the Earth's primitive mantle, *Geochim. Cosmochim. Acta*, 46, 176–192.
- Volodichev, O. A. (1990), *Belomorian Complex in Karelia: Geology and Petrology* (in Russian), 245 pp., Nauka, Leningrad.
- Zinger, T. F., J. Gotze, O. A. Levchenkov, et al. (1996), Zircon in polydeformed and metamorphosed Precambrian granitoids from the White sea tectonic zone, Russia: morphology, cathodoluminescence, and U–Pb chronology, *Int. Geol. Rev.*, 38, 57–73.

---

E. V. Sharkov, I. S. Krassivskaya, and A. V. Chistyakov, Institute of Geology of Ore Deposits, Petrography, Mineralogy, and Geochemistry (IGEM), Russian Academy of Sciences, Staromon-etnyi per. 35, Moscow, 109017 Russia e-mail: sharkovigem.ru

(Received 7 May 2004)